Nucl. Phys. B 997 (2023) 116386

Contents lists available at ScienceDirect

Nuclear Physics, Section B

journal homepage: www.elsevier.com/locate/nuclphysb

Quantum Field Theory and Statistical Systems

Contour-time approach to the disordered Bose-Hubbard model in the strong coupling regime

Ali Mokhtari-Jazi [a,*], Matthew R.C. Fitzpatrick [b], Malcolm P. Kennett [a]

[a] Department of Physics, Simon Fraser University, Burnaby, V5A 1S6, British Columbia, Canada
[b] Department of Physics, University of Victoria, Victoria, V8P 5C2, British Columbia, Canada

ARTICLE INFO

Editor: Hubert Saleur

ABSTRACT

There has been considerable interest in the disordered Bose Hubbard model (BHM) in recent years, particularly in the context of thermalization and many-body localization. We develop a two-particle irreducible (2PI) strong-coupling approach to the disordered BHM that allows us to treat both equilibrium and out-of-equilibrium situations. We obtain equations of motion for spatio-temporal correlations and explore their equilibrium solutions. We study the equilibrium phase diagram as a function of disorder strength and discuss applications of the formalism to out-of-equilibrium situations. We also note that the disorder strengths where the emergence of non-ergodic dynamics was observed in a recent experiment [Choi et al. (2016) [61]] appear to correspond to the Mott insulator – Bose Glass phase boundary.

Contents

* Corresponding author.
E-mail address: ama150@sfu.ca (A. Mokhtari-Jazi).

https://doi.org/10.1016/j.nuclphysb.2023.116386
Received 23 August 2023; Received in revised form 17 October 2023; Accepted 31 October 2023

Available online 8 November 2023

1. Introduction

Isolated strongly interacting quantum systems with quenched disorder may fail to thermalize and enter a phase in which the entire spectrum is composed of localized states [1,2]. Such many-body localized (MBL) states have been studied intensively in recent years [3–40]. In addition to their interest from a fundamental point of view, MBL states have also been suggested as having potential for use as quantum memories.

Aside from perturbative calculations [2,41–43] most of the evidence for MBL states comes from numerical calculations in one dimension [4–9,11,13,15–19,23,24,26,44,45]. Imbrie [21,22] has also provided rigorous arguments for the existence of MBL in one dimension under reasonable assumptions, although recent work has raised the question of whether particles are fully localized [34,39,40] or whether it is possible to reach large enough system sizes to study the MBL phase [32]. In dimensions higher than one, which is beyond the reach of many numerically exact methods, the situation is less clear and there is theoretical evidence and arguments for and against MBL [3,46–58].

Experimentally, there are indications of localization in disordered, interacting many body cold atom systems in optical lattices in two and higher dimensions [59–63]. Of particular interest for our work is the experiment by Choi et al. [61], in which the relaxation dynamics of disordered bosons in a two dimensional optical lattice were studied. Starting from an initial condition in which all of the atoms were localized on one side of a trap, Choi et al. observed the imbalance as a function of time and found that beyond a critical disorder strength, the system failed to thermalize in the time window of their experiment. Yan et al. [64] applied Gutzwiller mean-field theory (GMFT) to the two-dimensional disordered Bose Hubbard model and were able to reproduce the main experimental results, even though GMFT is unable to capture MBL, raising the possibility that the experiments probe glassy dynamics rather than MBL. This highlights the need to develop theoretical methods to investigate the out-of-equilibrium dynamics of the disordered Bose Hubbard model in dimensions greater than one.

There has been considerable study of the out-of-equilibrium dynamics of the Bose-Hubbard model realized in optical lattices [65–73]. In order to obtain spatial as well as temporal information, correlations are of particular interest, and a variety of methods, such as exact diagonalization (ED) and time-dependent density-matrix renormalization-group methods (t-DMRG) have been used in one dimension [74–83]. In two dimensions, where many of these approaches become less effective, methods for calculating correlations include perturbative corrections to Gutzwiller mean-field theory [84–87], time-dependent variational Monte Carlo [88], doublon-holon pair theories [89] and tensor network methods [90].

An alternative approach has been developed by two of us that is based on a two particle irreducible (2PI) out-of-equilibrium strong coupling approach to the BHM (2PISC) [91–95]. This approach allows the treatment of the dynamics of the order parameter and correlation functions on an equal footing and we have previously used it to demonstrate excellent agreement [96] with experiments investigating the spreading of correlations for bosons in optical lattices in one and two dimensions [78,97]. It also has the attractive feature that it allows for the inclusion of disorder averaging, which we make use of to study the disordered Bose-Hubbard model.

The presence of disorder in the BHM can lead to an additional phase in between the superfluid and Mott insulator, the Bose glass [98], and can reduce the size of the Mott lobes [98,99]. The experiments by Choi et al. [61] have focused attention on the out-of-equilibrium dynamics of the disordered Bose Hubbard model and both many-body localization and glassiness for bosons in one [100–104] and two or more dimensions [53,57,64,102,105–111]. This activity motivates our extension of the 2PISC formalism for the BHM to include disorder to provide an additional route to investigate the out-of-equilibrium dynamics of the disordered BHM.

The main result of this paper is that we develop a 2PI framework that allows us to treat both the equilibrium and out-of-equilibrium behavior of the disordered Bose Hubbard model. This allows us to obtain equations of motion for the superfluid order parameter and spatio-temporal correlations. We obtain solutions of these equations in the equilibrium case and investigate the Mott insulator phase boundary as a function of disorder strength and calculate the collective excitation spectrum both in and outside the Mott phase. We find that our results compare favorably with quantum Monte Carlo (QMC) simulations in two [112] and three [113] dimensions. We also note that the disorder strengths at which Ref. [61] found the emergence of non-ergodic dynamics appear to correspond to the Mott insulator – Bose glass phase boundary.

This paper is structured as follows: in Sec. 2 we introduce the disordered Bose Hubbard model and formalism, deriving an effective theory. We use our effective theory to obtain 2PI equations of motion which we then solve for equilibrium properties of the model in Sec. 3. We conclude and discuss our results in Sec. 4.

2. Model and formalism

In this section, we introduce the disordered Bose Hubbard model and discuss the generalization of the strong-coupling approach developed in Refs. [91,92,114] for the standard BHM to the disordered case allowing for both equilibrium and out-of-equilibrium behavior. The Hamiltonian for the disordered BHM is

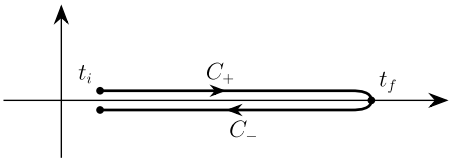

Fig. 1. Contour for a system initially prepared at time t_i. t_f is the maximum real-time considered in the problem, which may be set to $t_f \to \infty$ without loss of generality.

$$\hat{H}^{\rm dis}_{\rm BHM}(\epsilon) = \hat{H}_J + \hat{H}_0 + \hat{H}_\epsilon, \tag{1}$$

where

$$\hat{H}_J = -\sum_{\langle \vec{r}_1, \vec{r}_2 \rangle} J_{\vec{r}_1\vec{r}_2} \left(\hat{a}^\dagger_{\vec{r}_1} \hat{a}_{\vec{r}_2} + \hat{a}_{\vec{r}_2} \hat{a}^\dagger_{\vec{r}_1} \right), \tag{2}$$

$$\hat{H}_0 = \frac{U}{2} \sum_{\vec{r}} \hat{n}_{\vec{r}} \left(\hat{n}_{\vec{r}} - 1 \right) + \sum_{\vec{r}} \left(V_{\vec{r}} - \mu \right) \hat{n}_{\vec{r}}, \tag{3}$$

$$\hat{H}_\epsilon = \sum_{\vec{r}} \epsilon_{\vec{r}}\, \hat{n}_{\vec{r}}, \tag{4}$$

with $\hat{a}^\dagger_{\vec{r}}$ and $\hat{a}_{\vec{r}}$ annihilation and creation operators for bosons on lattice site $\vec{r}$ respectively, $\hat{n}_{\vec{r}} \equiv \hat{a}^\dagger_{\vec{r}} \hat{a}_{\vec{r}}$ the number operator, U the interaction strength, $V_{\vec{r}}$ a harmonic trapping potential, μ the chemical potential, and ϵ_r an on-site disorder potential. The hopping strength is $J_{\vec{r}_1\vec{r}_2}$ and we allow the possibility that this is time dependent, as is in the case of some out of equilibrium cold atom experiments. The disorder potential is drawn from a Gaussian distribution

$$\mathcal{P}\left[\epsilon_{\vec{r}}\right] = \sqrt{\frac{4\ln 2}{\pi \Delta^2_\epsilon}}\, e^{-\frac{4(\ln 2)\epsilon^2_{\vec{r}}}{\Delta^2_\epsilon}}, \tag{5}$$

with Δ_ϵ being the full-width at half maximum for the distribution. The choice of a Gaussian disorder distribution is made for comparison with experiment [61] and for analytic convenience. The notation $\langle \vec{r}_1, \vec{r}_2 \rangle$ indicates a sum over nearest neighbors only.

In the strong coupling approach to the BHM that we extend to the disordered case here, one starts from the Hamiltonian and then obtains a generating functional. Then, one performs two Hubbard-Stratonovich transformations on the hopping term, which gives an action which allows for expansion about the strong coupling limit [114]. This approach was generalized to an out of equilibrium Contour formalism in Ref. [91]. From the action of the effective theory thus obtained, one can determine the 2PI equations of motion that allow calculation of excitations, correlations and phase boundaries [92,93].

2.1. Contour-time formalism

The general formalism that we discuss and adopt in this paper was developed in a previous paper by two of us; we refer the reader to Ref. [92] for further details on the formalism. We use the contour-time formalism [115–120], which replaces the notion of real time along the real line with contour time, a complex valued time on a contour in the complex plane. Furthermore, an appropriate choice of contour is particularly attractive for studying disordered systems as it eliminates the need to use replicas in carrying out the average over the quenched disorder because the generating functional is automatically normalized to $Z = 1$ [121,122]. For systems initially prepared in out-of-equilibrium states, one can work with a contour C of the form illustrated in Fig. 1. A popular alternative to this contour is the Schwinger-Keldysh (SK) closed-time path [115,116] which is also suitable for certain out-of-equilibrium problems. However, unlike contour C, the SK contour ignores transient phenomena and, more importantly, information about the initial state. Given that we are interested in comparing long-time density profiles with that of the initial state, contour C is a more appropriate choice. We assume that the dynamics due to the disordered potential are not correlated with the initial state.

2.2. Contour-ordered Green's functions

In deriving our effective theory of the disordered BHM, we calculate various contour-ordered Green's functions (COGFs). We define the n-point COGF as [120]

$$\begin{aligned} G^{a_1\ldots a_n}_{\vec{r}_1\ldots\vec{r}_n}\left(\tau_1,\ldots,\tau_n;\epsilon\right) &\equiv (-i)^{n-1}\,\mathrm{Tr}\left\{\hat{\rho}_i T_C\left[\hat{a}^{a_1}_{\vec{r}_1}\left(\tau_1;\epsilon\right)\ldots\hat{a}^{a_n}_{\vec{r}_n}\left(\tau_n;\epsilon\right)\right]\right\} \\ &\equiv (-i)^{n-1}\left\langle T_C\left[\hat{a}^{a_1}_{\vec{r}_1}\left(\tau_1;\epsilon\right)\ldots\hat{a}^{a_n}_{\vec{r}_n}\left(\tau_n;\epsilon\right)\right]\right\rangle_{\hat{\rho}_i}, \end{aligned} \tag{6}$$

where $\hat{\rho}_i$ is the state operator representing the initial state of the system, and the a_i upper indices are defined such that

$$\hat{a}^1_{\vec{r}} \equiv \hat{a}_{\vec{r}}, \quad \hat{a}^2_{\vec{r}} \equiv \hat{a}^\dagger_{\vec{r}}, \tag{7}$$

and $\hat{a}^a_{\vec{r}}(\tau;\epsilon)$ are the bosonic fields in the Heisenberg picture with respect to $\hat{H}_{\rm BHM}(\tau;\epsilon)$ [Eq. (1)]

$$\hat{a}^a_{\vec{r}}(\tau;\epsilon) = U_C\left(\tau_i,\tau;\epsilon\right)\hat{a}^a_{\vec{r}}\,U_C\left(\tau,\tau_i;\epsilon\right), \tag{8}$$

$$U_C\left(\tau,\tau';\epsilon\right) = \begin{cases} T_C\left[e^{-i\int_{C(\tau,\tau')}d\tau''\hat{H}^{\rm dis}_{\rm BHM}(\tau'';\epsilon)}\right], & \text{if } \tau \text{ later than } \tau', \\ T_C\left[e^{i\int_{C(\tau,\tau')}d\tau''\hat{H}^{\rm dis}_{\rm BHM}(\tau'';\epsilon)}\right], & \text{if } \tau' \text{ later than } \tau. \end{cases} \tag{9}$$

Here we have introduced explicitly the complex contour time argument τ, the sub-contour $C\left(\tau,\tau'\right)$ which goes from τ to τ' along the contour C, and the contour time ordering operator T_C, which orders strings of operators according to their position on the contour, with operators at earlier contour times placed to the right.

Given the somewhat cumbersome notation in expressions such as that in Eq. (6), we make extensive use of a compact notation where we write an arbitrary function X as

$$X^{a_1\ldots a_n}_{\vec{r}_1\ldots\vec{r}_n,\tau_1\ldots\tau_n;\epsilon} \equiv X^{a_1\ldots a_n}_{\vec{r}_1\ldots\vec{r}_n}\left(\tau_1\ldots\tau_n;\epsilon\right), \tag{10}$$

and introduce the following implicit summation convention

$$X^a_{\tau;\epsilon}Y^{\overline{a}}_{\tau;\epsilon} = \sum_{a_1a_2}\int_C d\tau\sigma_1^{a_1a_2}X^{a_1}(\tau;\epsilon)\,Y^{a_2}(\tau;\epsilon), \tag{11}$$

where σ_i is the $i^{\rm th}$ Pauli matrix, $\overline{1}=2$ and $\overline{2}=1$. Note that we only include the ϵ parameter in Eq. (10) if the function X depends on the disorder configuration.

2.3. Generating functional $\mathcal{Z}[f;\epsilon]$

The COGFs above can be derived from a generating functional $\mathcal{Z}[f;\epsilon]$, which can be cast in the following path integral form [91,92,94,118]:

$$\mathcal{Z}[f;\epsilon] = \int[\mathcal{D}a]\left\langle\mathbf{a}\left(\tau_i\right)\left|\hat{\rho}_i(\epsilon)\right|\mathbf{a}\left(\tau_f\right)\right\rangle e^{-\frac{1}{2}\left\{\mathbf{a}\left(\tau_i\right).\mathbf{a}\left(\tau_i\right)+\mathbf{a}\left(\tau_f\right).\mathbf{a}\left(\tau_f\right)\right\}}e^{iS[a;\epsilon]+iS_f[a]}, \tag{12}$$

where τ_i and τ_f are the initial and final points on the contour, chosen to be the same as C in Fig. 1, and $S[a;\epsilon]$ is the action for the disordered BHM

$$S[a;\epsilon] = S_J[a] + S_0[a] + S_\epsilon[a], \tag{13}$$

with

$$S_J[a] = \frac{1}{2!}\sum_{\vec{r}_1\vec{r}_2}\left\{2J^{a_1a_2}_{\vec{r}_1\vec{r}_2,\tau_1\tau_2}\right\}a^{\overline{a_1}}_{\vec{r}_1,\tau_1}a^{\overline{a_2}}_{\vec{r}_2,\tau_2}, \tag{14}$$

$$\begin{aligned} S_0[a] = {} & \frac{1}{2!}\sum_{\vec{r}}a^{\overline{a_1}}_{\vec{r},\tau_1}\left\{-\partial^{a_1a_2}_{\tau_1\tau_2}-\left\{V_{\vec{r}}-\mu\right\}\zeta^{a_1a_2}_{\tau_1\tau_2}\right\}a^{\overline{a_2}}_{\vec{r},\tau_2} \\ & -\frac{1}{4!}\sum_{\vec{r}}\left\{U\zeta^{a_1a_2a_3a_4}_{\tau_1\tau_2\tau_3\tau_4}\right\}a^{\overline{a_1}}_{\vec{r},\tau_1}a^{\overline{a_2}}_{\vec{r},\tau_2}a^{\overline{a_3}}_{\vec{r},\tau_3}a^{\overline{a_4}}_{\vec{r},\tau_4}, \end{aligned} \tag{15}$$

$$S_\epsilon[a] = \frac{1}{2!}\sum_{\vec{r}}\left\{-\epsilon_{\vec{r}}\,\zeta^{a_1a_2}_{\tau_1\tau_2}\right\}a^{\overline{a_1}}_{\vec{r},\tau_1}a^{\overline{a_2}}_{\vec{r},\tau_2}, \tag{16}$$

with

$$J^{a_1a_2}_{\vec{r}_1\vec{r}_2,\tau_1\tau_2} = J_{\vec{r}_1\vec{r}_2}\zeta^{a_1a_2}_{\tau_1\tau_2}, \tag{17}$$

$$\zeta^{a_1a_2}_{\tau_1\tau_2} = \delta_{\tau_1\tau_2}\sigma_1^{a_1a_2}, \tag{18}$$

and

$$\zeta^{a_1a_2a_3a_4}_{\tau_1\tau_2\tau_3\tau_4} = 2\delta_{\tau_1\tau_2}\delta_{\tau_2\tau_3}\delta_{\tau_3\tau_4}\sigma^{a_1a_2a_3a_4}, \tag{19}$$

where

$$\sigma^{a_1a_2a_3a_4} = \begin{cases} 1, & \text{if } \left\{a_m\right\}_{m=1}^4 \in P(\{1,1,2,2\}), \\ 0, & \text{otherwise.} \end{cases} \tag{20}$$

$S_f[a]$ is the source term

$$S_f[a] = \sum_{\vec{r}} f^{a}_{\vec{r},\tau} a^{\overline{a}}_{\vec{r},\tau}, \tag{21}$$

and $\int [Da]$ is the coherent-state measure. Note that in the path-integral formalism $a^1_{\vec{r}} = a_{\vec{r}}$ and $a^2_{\vec{r}} = a^*_{\vec{r}}$. In this formalism, we can rewrite averages of the form $\langle T_C[\ldots]\rangle_{\hat{\rho}_i}$ as follows

$$\left\langle T_C\left[\hat{a}^{a_1}_{\vec{r}_1,\tau_1;\epsilon}\ldots\hat{a}^{a_n}_{\vec{r}_n,\tau_n;\epsilon}\right]\right\rangle_{\hat{\rho}_i} \equiv \left\langle a^{a_1}_{\vec{r}_1,\tau_1}\ldots a^{a_n}_{\vec{r}_n,\tau_n}\right\rangle_S, \tag{22}$$

where contour ordering is now implicit in the path integral representation [123]. Occasionally, we drop the action subscript $\langle\ldots\rangle_S \to \langle\ldots\rangle$ for brevity.

To derive the COGFs in Eq. (6) from $\mathcal{Z}[f;\epsilon]$, we take appropriate functional derivatives with respect to the sources and set the sources to zero afterwards

$$G^{a_1\ldots a_n}_{\vec{r}_1\ldots\vec{r}_n,\tau_1\ldots\tau_{n;\epsilon}} = i(-1)^n \left.\frac{\delta^n\mathcal{Z}[f;\epsilon]}{\delta f^{\overline{a_1}}_{\vec{r}_1,\tau_1}\ldots\delta f^{\overline{a_n}}_{\vec{r}_n,\tau_n}}\right|_{f\to 0}. \tag{23}$$

2.4. Disorder averaging

We are ultimately interested in calculating disorder averaged COGFs

$$\check{G}^{a_1\ldots a_n}_{\vec{r}_1\ldots\vec{r}_n,\tau_1\ldots\tau_n} = \left(\prod_{\vec{r}}\int_{-\infty}^{\infty} d\epsilon_{\vec{r}}\,\mathcal{P}\left[\epsilon_{\vec{r}}\right]\right) G^{a_1\ldots a_n}_{\vec{r}_1\ldots\vec{r}_n,\tau_1\ldots\tau_{n;\epsilon}}, \tag{24}$$

where for a quantity θ we denote the disorder average $\check{\theta}$ with a carat. Using Eq. (23) we can determine an expression for calculating the disorder-averaged COGFs:

$$\check{G}^{a_1\ldots a_n}_{\vec{r}_1\ldots\vec{r}_n,\tau_1\ldots\tau_n} = i(-1)^n \left.\frac{\delta^n\check{\mathcal{Z}}[f]}{\delta f^{\overline{a_1}}_{\vec{r}_1,\tau_1}\ldots\delta f^{\overline{a_n}}_{\vec{r}_n,\tau_n}}\right|_{f\to 0}, \tag{25}$$

where $\check{\mathcal{Z}}[f]$ is the disorder-average of $\mathcal{Z}[f;\epsilon]$.

2.5. Effective theory of the disordered BHM

We develop an effective theory that is suitable for studying the dynamics of the disordered BHM in the strong coupling regime. The approach can be outlined as follows: first we calculate the disorder average of $\mathcal{Z}[f;\epsilon]$, and decouple the resulting quartic term with a Hubbard-Stratonovich transformation which introduces an additional field Q. This gives us an effective theory $S^{\rm dis}_{\rm eff}$ in terms of the original a-fields and Q for which we follow the same procedure as in the clean case, but with extra terms that arise from the disorder. The resulting effective strong coupling theory introduces two auxiliary fields z and $\mathcal{Q}$. We derive identities relating the correlators of these two auxiliary fields to those of the original a-fields. One can then apply a two-particle irreducible effective action approach [124] to the effective theory to obtain equations of motion for the correlation functions.

We begin by performing the disorder average of $\mathcal{Z}[f;\epsilon]$

$$\check{\mathcal{Z}}[f] = \int [Da]\left\langle \mathbf{a}(\tau_i)\left|\hat{\rho}_i\right|\mathbf{a}(\tau_f)\right\rangle e^{-\frac{1}{2}\{\mathbf{a}(\tau_i).\mathbf{a}(\tau_i)+\mathbf{a}(\tau_f).\mathbf{a}(\tau_f)\}} e^{iS_\Delta[a]} e^{iS_J[a]+iS_0[a]+iS_f[a]}, \tag{26}$$

where

$$e^{iS_\Delta[a]} = \left\{\prod_{\vec{r}}\int_{-\infty}^{\infty} d\epsilon_{\vec{r}}\,\mathcal{P}\left[\epsilon_{\vec{r}}\right]\right\} e^{iS_\epsilon[a]}. \tag{27}$$

Next, using Eqs. (5) and (16) we calculate $e^{iS_\Delta[a]}$:

$$\begin{aligned} e^{iS_\Delta[a]} &= \prod_{\vec{r}}\int_{-\infty}^{\infty} d\epsilon_{\vec{r}}\,\mathcal{P}\left[\epsilon_{\vec{r}}\right]\exp\left\{\frac{i}{2!}\left(-\epsilon_{\vec{r}}\,\zeta^{a_1a_2}_{\tau_1\tau_2}\right)a^{\overline{a_1}}_{\vec{r},\tau_1}a^{\overline{a_2}}_{\vec{r},\tau_2}\right\} \\ &= \exp\left\{\frac{i}{2!}\sum_{\vec{r}}\left(-\frac{1}{4}M^{[\![a_1a_2]\!][\![a_3a_4]\!]}_{[\![\tau_1\tau_2]\!][\![\tau_3\tau_4]\!]}\right)a^{\overline{a_1}}_{\vec{r},\tau_1}a^{\overline{a_2}}_{\vec{r},\tau_2}a^{\overline{a_3}}_{\vec{r},\tau_3}a^{\overline{a_4}}_{\vec{r},\tau_4}\right\}, \end{aligned} \tag{28}$$

where

$$M^{[\![a_1a_2]\!][\![a_3a_4]\!]}_{[\![\tau_1\tau_2]\!][\![\tau_3\tau_4]\!]} \equiv -i\widetilde{\Delta}^2_\epsilon\zeta^{a_1a_3}_{\tau_1\tau_3}\zeta^{a_2a_4}_{\tau_2\tau_4}, \tag{29}$$

and

$$\widetilde{\Delta}_{\epsilon}^{2}=\frac{\Delta_{\epsilon}^{2}}{8\ln 2}. \tag{30}$$

To decouple the quartic a-field term in Eq. (30), we perform a Hubbard-Stratonovich transformation (similarly to e.g. Ref. [125])

$$\begin{aligned} e^{iS_{\Delta}[a]} &= \int [DQ]\exp\left\{\frac{i}{2!}\sum_{\vec{r}}\left[M^{-1}\right]^{[\![a_1a_2]\!][\![a_3a_4]\!]}_{[\![\tau_1\tau_2]\!][\![\tau_3\tau_4]\!]}Q^{\overline{a_1a_2}}_{\vec{r}\vec{r},\tau_1\tau_2}Q^{\overline{a_3a_4}}_{\vec{r}\vec{r},\tau_3\tau_4}+\frac{i}{2!}\sum_{\vec{r}}Q^{a_1a_2}_{\vec{r}\vec{r},\tau_1\tau_2}a^{\overline{a_1}}_{\vec{r},\tau_1}a^{\overline{a_2}}_{\vec{r},\tau_2}\right\} \\ &\equiv \int [DQ]\,e^{iS_{M^{-1}}[Q]+iS_{Q}[a]}, \end{aligned} \tag{31}$$

where

$$\left[M^{-1}\right]^{[\![a_1a_2]\!][\![a_3a_4]\!]}_{[\![\tau_1\tau_2]\!][\![\tau_3\tau_4]\!]}\equiv\frac{i}{\widetilde{\Delta}_{\epsilon}^{2}}\zeta^{a_1a_3}_{\tau_1\tau_3}\zeta^{a_2a_4}_{\tau_2\tau_4}, \tag{32}$$

$$S_{M^{-1}}[Q]=\frac{1}{2!}\sum_{\vec{r}}\left[M^{-1}\right]^{[\![a_1a_2]\!][\![a_3a_4]\!]}_{[\![\tau_1\tau_2]\!][\![\tau_3\tau_4]\!]}Q^{\overline{a_1a_2}}_{\vec{r}\vec{r},\tau_1\tau_2}Q^{\overline{a_3a_4}}_{\vec{r}\vec{r},\tau_3\tau_4}, \tag{33}$$

and

$$S_{Q}[a]=\frac{1}{2!}\sum_{\vec{r}}Q^{a_1a_2}_{\vec{r}\vec{r},\tau_1\tau_2}a^{\overline{a_1}}_{\vec{r},\tau_1}a^{\overline{a_2}}_{\vec{r},\tau_2}, \tag{34}$$

and Q is an auxiliary field introduced by the transformation.

At this point, the generating functional $\mathcal{Z}[f,K]$ can be written as

$$\begin{aligned} \check{\mathcal{Z}}[f] &= \int [Da]\left\langle \mathbf{a}(\tau_i)\left|\hat{\rho}_i\right|\mathbf{a}(\tau_f)\right\rangle e^{-\frac{1}{2}\{\mathbf{a}(\tau_i).\mathbf{a}(\tau_i)+\mathbf{a}(\tau_f).\mathbf{a}(\tau_f)\}} \\ &\quad\times\int [DQ]\,e^{i\left(S_J[a]+S_0[a]+S_{M^{-1}}[Q]+S_f[a]+S_Q[a]\right)}. \end{aligned} \tag{35}$$

Next, following Refs. [91,92,114,126], we decouple the hopping term by performing a Hubbard-Stratonovich transformation on the hopping term

$$\begin{aligned} \mathcal{Z}[f] &= \int [Da]\left\langle \mathbf{a}(\tau_i)\left|\hat{\rho}_i\right|\mathbf{a}(\tau_f)\right\rangle e^{-\frac{1}{2}\{\mathbf{a}(\tau_i).\mathbf{a}(\tau_i)+\mathbf{a}(\tau_f).\mathbf{a}(\tau_f)\}} \\ &\quad\times\int [DQ]\int [D\psi]\,e^{i\left(-S_{J^{-1}}[\psi]+S_0[a]+S_{M^{-1}}[Q]-S_{\psi}[a]+S_f[a]+S_Q[a]\right)}, \end{aligned} \tag{36}$$

where

$$S_{J^{-1}}[\psi]=\frac{1}{2!}\sum_{\vec{r}_1\vec{r}_2}\left(\frac{1}{2}\left[J^{-1}\right]^{a_1a_2}_{\vec{r}_1\vec{r}_2,\tau_1\tau_2}\right)\psi^{\overline{a_1}}_{\vec{r}_1,\tau_1}\psi^{\overline{a_2}}_{\vec{r}_2,\tau_2}, \tag{37}$$

with

$$S_{\psi}[a]=\sum_{\vec{r}}\psi^{a}_{\vec{r},\tau}a^{\overline{a}}_{\vec{r},\tau}, \tag{38}$$

and ψ is another auxiliary field. By making a field substitution, $\psi^{a}_{\vec{r},\tau}\to-\psi^{a}_{\vec{r},\tau}+f^{a}_{\vec{r},\tau}$, and rearranging terms in Eq. (36) we get

$$\check{\mathcal{Z}}[f]=\int [DQ][D\psi]\,e^{i\left(-S_{J^{-1}}[\psi-f]+S_{M^{-1}}[Q]\right)}\mathcal{Z}_0[\psi,Q], \tag{39}$$

where

$$\begin{aligned} \mathcal{Z}_0[\psi,Q] &\equiv e^{iW_0[\psi,Q]} \\ &= \int [Da]\left\langle \mathbf{a}(\tau_i)\left|\hat{\rho}_i\right|\mathbf{a}(\tau_f)\right\rangle e^{-\frac{1}{2}\{\mathbf{a}(\tau_i).\mathbf{a}(\tau_i)+\mathbf{a}(\tau_f).\mathbf{a}(\tau_f)\}}e^{i(S_0[a]+S_{\psi}[a]+S_Q[a])}. \end{aligned} \tag{40}$$

In this context ψ and Q take the same form as f and K in the 2PI generating functionals introduced in Ref. [92], i.e. by taking functional derivatives of $\mathcal{Z}_0[\psi,Q]$ (or $W_0[\psi,Q]$) with respect to ψ and Q one can generate all n-point COGFs (or CCOGFs). In this case the generating functionals $\mathcal{Z}_0[\psi,Q]$ and $W_0[\psi,Q]$ are governed by a different theory than that introduced in Ref. [92].

$W_0[\psi,Q]$ generates all the n-point CCOGFs in the limit of zero disorder and hopping for a system prepared in the initial state $\hat{\rho}_i$

$$\mathcal{G}^{a_1\ldots a_n,c}_{\vec{r}_1\ldots\vec{r}_n,\tau_1\ldots\tau_n}=(-1)^{n-1}\left.\frac{\delta^n W_0[\psi,Q]}{\delta\psi^{\overline{a_1}}_{\vec{r}_1,\tau_1}\ldots\delta\psi^{\overline{a_n}}_{\vec{r}_n,\tau_n}}\right|_{\psi,Q\to 0}, \tag{41}$$

as well as a set of generalized CCOGFs defined by:

$$\mathcal{G}^{a_1\ldots a_{n_1}}_{\vec{r}_1\ldots\vec{r}_{n_1}}\left[\!\left[a'_1a''_1\right]\!\right]\ldots\left[\!\left[a'_{n_2}a''_{n_2}\right]\!\right],c \\ \left[\!\left[\vec{r}'_1\vec{r}''_1\right]\!\right]\ldots\left[\!\left[\vec{r}'_{n_2}\vec{r}''_{n_2}\right]\!\right],\tau_1\ldots\tau_{n_1}\left[\!\left[\tau'_1\tau''_1\right]\!\right]\ldots\left[\!\left[\tau'_{n_2}\tau''_{n_2}\right]\!\right]$$

$$\equiv-(-1)^{n_1}(2i)^{n_2}\left.\frac{\delta^{n_1+n_2}W_0[\psi,\mathcal{Q}]}{\delta\psi^{\overline{a_1}}_{\vec{r}_1,\tau_1}\ldots\delta\psi^{\overline{a_{n_1}}}_{\vec{r}_{n_1},\tau_{n_1}}\delta\mathcal{Q}^{\overline{a'_1a''_1}}_{\vec{r}'_1\vec{r}''_1,\tau'_1\tau''_1}\ldots\delta\mathcal{Q}^{\overline{a'_{n_2}a''_{n_2}}}_{\vec{r}'_{n_2}\vec{r}''_{n_2},\tau'_{n_2}\tau''_{n_2}}}\right|_{\psi,\mathcal{Q}\to0}. \tag{42}$$

These functions are connected in a particular sense: indices that are paired inside a pair of brackets $[\![\ldots]\!]$ should be thought of as indices belonging to a single field. If we assume an initial state of the form

$$\hat{\rho}_i=\otimes_{\vec{r}}\left|n_{i,\vec{r}}\right\rangle\left\langle n_{i,\vec{r}}\right|, \tag{43}$$

the CCOGFs defined in Eqs. (41) and (42) vanish unless all site indices are equal. Moreover, when Eq. (43) holds, correlators of the form $\left\langle a^{a_1}_{\vec{r}_1,\tau_1}\ldots a^{a_n}_{\vec{r}_n,\tau_n}\right\rangle_{S_0}$ vanish unless the number of a^*-fields equals the number of a-fields. By inverting Eq. (42) we may rewrite W_0 as

$$W_0[\psi,\mathcal{Q}]=-\Theta\left(n_1+n_2-1/2\right)\sum_{n_1=0}^{\infty}\sum_{n_2=0}^{\infty}\frac{(-i)^{n_2}}{(2n_1)!n_2!2^{n_2}}\prod_{m_1=1}^{2n_1}\left(\sum_{r_{m_1}}\right)\prod_{m_2=1}^{n_2}\left(\sum_{r'_{m_2}r''_{m_2}}\right) \\ \times\mathcal{G}^{a_1\ldots a_{2n_1}}_{\vec{r}_1\ldots\vec{r}_{2n_1}}\left[\!\left[a'_1a''_1\right]\!\right]\ldots\left[\!\left[a'_{n_2}a''_{n_2}\right]\!\right],c \\ \left[\!\left[\vec{r}'_1\vec{r}''_1\right]\!\right]\ldots\left[\!\left[\vec{r}'_{n_2}\vec{r}''_{n_2}\right]\!\right],\tau_1\ldots\tau_{2n_1}\left[\!\left[\tau'_1\tau''_1\right]\!\right]\ldots\left[\!\left[\tau'_{n_2}\tau''_{n_2}\right]\!\right] \\ \times\psi^{\overline{a_1}}_{r_1,\tau_1}\ldots\psi^{\overline{a_{2n_1}}}_{r_{2n_1},\tau_{2n_1}}\mathcal{Q}^{\overline{a'_1a''_1}}_{r'_1r''_1,\tau'_1\tau''_1}\ldots\mathcal{Q}^{\overline{a'_{n_2}a''_{n_2}}}_{r'_{n_2}r''_{n_2},\tau'_{n_2}\tau''_{n_2}}, \tag{44}$$

where $\Theta(x)$ is the Heaviside function. Following Refs. [91,92,114,126], we perform a second Hubbard-Stratonovich transformation to decouple the inverse hopping term such that

$$\check{\mathcal{Z}}[f]=\int[\mathcal{D}z]\int[\mathcal{D}\mathcal{Q}]\,e^{i\left(S_J[z]+S_{M^{-1}}[\mathcal{Q}]+\widetilde{W}_0[z,\mathcal{Q}]+S_f[z]\right)}, \tag{45}$$

where

$$e^{i\widetilde{W}_0[z,\mathcal{Q}]}=\int[\mathcal{D}\psi]\,e^{i\left(W_0[\psi,\mathcal{Q}]+S_z[\psi]\right)}, \tag{46}$$

with

$$S_z[\psi]=\sum_{\vec{r}}z^a_{\vec{r},\tau}\psi^{\overline{a}}_{\vec{r},\tau}. \tag{47}$$

The effective theory is obtained by adding all of the action terms excluding sources

$$S^{\mathrm{dis}}_{\mathrm{eff}}[z,\mathcal{Q}]=S_J[z]+S_{M^{-1}}[\mathcal{Q}]+\widetilde{W}_0[z,\mathcal{Q}]. \tag{48}$$

We next perform a cumulant expansion of $\widetilde{W}_0$, similar to that found in Refs. [91,92,114,126] although the calculation is more complicated in the disordered case.

Even in the compact notation we introduced in Sec. 2.2, the resulting expression for the effective theory is quite cumbersome to write out. We therefore condense the notation further such that

$$X^{\chi_i}=\begin{pmatrix}X^{z_i}\\ X^{\mathcal{Q}_{i'i''}}\end{pmatrix} \\ =\begin{pmatrix}X^{a_i}_{\vec{r}_i,\tau_i}\\ X^{a'_ia''_i}_{\vec{r}'_i\vec{r}''_i,\tau'_i\tau''_i}\end{pmatrix}, \tag{49}$$

$$X^{\chi_i}Y^{\chi_i}=X^{z_i}Y^{z_i}+X^{\mathcal{Q}_{i'i''}}Y^{\mathcal{Q}_{i'i''}} \\ =\sum_{\vec{r}_i}X^{a_i}_{\vec{r}_i,\tau_i}Y^{\overline{a_i}}_{\vec{r}_i,\tau_i}+\sum_{\vec{r}'_i\vec{r}''_i}X^{a'_ia''_i}_{\vec{r}'_i\vec{r}''_i,\tau'_i\tau''_i}Y^{\overline{a'_ia''_i}}_{\vec{r}'_i\vec{r}''_i,\tau'_i\tau''_i}. \tag{50}$$

Using the above shorthand notation, the effective theory can be expressed as follows

$$S^{\mathrm{dis}}_{\mathrm{eff}}[\Phi]=\left(\frac{1}{2!}\left[g_0^{-1}\right]^{\chi_1\chi_2}\right)\Phi^{\chi_1}\Phi^{\chi_2}+\sum_{n=1}^{\infty}\frac{1}{n!}g^{\chi_1\cdots\chi_n}\Phi^{\chi_1}\ldots\Phi^{\chi_n}, \tag{51}$$

where

$$\Phi^{\chi_i} = \begin{pmatrix} z^{a_i}_{\vec{r}_i,\tau_i} \\ Q^{a_i' a_i''}_{\vec{r}_i' \vec{r}_i'', \tau_i' \tau_i''} \end{pmatrix}. \tag{52}$$

The couplings for quadratic terms in the theory are:

$$\left[g_0^{-1}\right]^{z_1 z_2} = \left[(\mathcal{G}^c)^{-1}\right]^{a_1 a_2}_{\vec{r}_1 \vec{r}_2, \tau_1 \tau_2}, \tag{53}$$

$$\left[g_0^{-1}\right]^{z_1 Q_{23}} = 0, \tag{54}$$

$$\left[g_0^{-1}\right]^{Q_{12} z_3} = 0, \tag{55}$$

$$\left[g_0^{-1}\right]^{Q_{12} Q_{34}} = \delta_{[\![\vec{r}_1 \vec{r}_2]\!][\![\vec{r}_3 \vec{r}_4]\!]} \left[M^{-1}\right]^{[\![a_1 a_2]\!][\![a_3 a_4]\!]}_{[\![\tau_1 \tau_2]\!][\![\tau_3 \tau_4]\!]}, \tag{56}$$

with

$$\delta_{[\![\vec{r}_1 \vec{r}_2]\!][\![\vec{r}_3 \vec{r}_4]\!]} = \begin{cases} 1, & \text{if } \vec{r}_1 = \vec{r}_2 = \vec{r}_3 = \vec{r}_4 \\ 0, & \text{otherwise} \end{cases}, \tag{57}$$

and the vertices $g^{\chi_1 \cdots \chi_n}$ are combinations of the CCOGFs generated from W_0. The presence of the contour ordering operator T_C in the CCOGFs leads to symmetry under permutations $\{p_1, \ldots, p_n\}$ of the sequence $\{1, \ldots, n\}$:

$$\left[g_0^{-1}\right]^{\chi_1 \chi_2} = \left[g_0^{-1}\right]^{\chi_{p_1} \chi_{p_2}}, \tag{58}$$

$$g^{\chi_1 \cdots \chi_n} = g^{\chi_{p_1} \cdots \chi_{p_n}}. \tag{59}$$

The action in Eq. (51) contains an infinite sum, therefore for practical calculations we truncate the action keeping only terms to order $\mathcal{O}[\psi^n Q^m]$ where $4 - 2m \geq n \geq 0$ and $2 \geq m \geq 0$. Out of these terms, the only non-vanishing terms (modulo index-permutations) are

$$g^{Q_{12}} = \frac{i}{2} \mathcal{G}^{[\![a_1 a_2]\!], c}_{[\![\vec{r}_1 \vec{r}_2]\!], [\![\tau_1 \tau_2]\!]} + \frac{1}{4} \mathcal{G}^{[\![a_1 a_2]\!] a_3 a_4, c}_{[\![\vec{r}_1 \vec{r}_2]\!] \vec{r}_3 \vec{r}_4, [\![\tau_1 \tau_2]\!] \tau_3 \tau_4} \left[(\mathcal{G}^c)^{-1}\right]^{\overline{a_3 a_4}}_{\vec{r}_3 \vec{r}_4, \tau_3 \tau_4}, \tag{60}$$

$$g^{z_1 z_2} = 2 J^{a_1 a_2}_{\vec{r}_1 \vec{r}_2, \tau_1 \tau_2} + \tilde{u}^{a_1 a_2}_{\vec{r}_1 \vec{r}_2, \tau_1 \tau_2}, \tag{61}$$

$$g^{Q_{12} Q_{34}} = \frac{1}{4} \mathcal{G}^{[\![a_1 a_2]\!][\![a_3 a_4]\!], c}_{[\![r_1 r_2]\!][\![r_3 r_4]\!], [\![\tau_1 \tau_2]\!][\![\tau_3 \tau_4]\!]}, \tag{62}$$

$$g^{z_1 z_2 Q_{34}} = \frac{1}{3} u^{a_1 a_2 [\![a_3 a_4]\!]}_{\vec{r}_1 \vec{r}_2 [\![\vec{r}_3 \vec{r}_4]\!], \tau_1 \tau_2 [\![\tau_3 \tau_4]\!]}, \tag{63}$$

$$g^{z_1 z_2 z_3 z_4} = u^{a_1 a_2 a_3 a_4}_{\vec{r}_1 \vec{r}_2 \vec{r}_3 \vec{r}_4, \tau_1 \tau_2 \tau_3 \tau_4}, \tag{64}$$

where

$$\tilde{u}^{a_1 a_2}_{\vec{r}_1 \vec{r}_2, \tau_1 \tau_2} = -\frac{1}{2!} \sum_{\vec{r}_3 \vec{r}_4} u^{a_1 a_2 a_3 a_4}_{\vec{r}_1 \vec{r}_2 \vec{r}_3 \vec{r}_4, \tau_1 \tau_2 \tau_3 \tau_4} \left\{ i \mathcal{G}^{\overline{a_3 a_4}, c}_{\vec{r}_3 \vec{r}_4, \tau_3 \tau_4} \right\}, \tag{65}$$

is an "anomalous" [126] term generated in the cumulant expansion which has an internal inverse bare propagator line. It is required to ensure that the 2PI equations of motion are correct in the atomic limit (see Ref. [92] for additional details). We also have

$$u^{a_1 a_2 [\![a_3 a_4]\!]}_{\vec{r}_1 \vec{r}_2 [\![\vec{r}_3 \vec{r}_4]\!], \tau_1 \tau_2 [\![\tau_3 \tau_4]\!]} \equiv \frac{3i}{2} \prod_{m=1}^{2} \left\{ \sum_{\vec{r}_m'} \left[(\mathcal{G}^c)^{-1}\right]^{a_m a_m'}_{\vec{r}_m \vec{r}_m', \tau_m \tau_m'} \right\} \mathcal{G}^{\overline{a_1' a_2'} [\![a_3 a_4]\!], c}_{\vec{r}_1' \vec{r}_2' [\![\vec{r}_3 \vec{r}_4]\!], \tau_1' \tau_2' [\![\tau_3 \tau_4]\!]}, \tag{66}$$

and

$$u^{a_1 a_2 a_3 a_4}_{\vec{r}_1 \vec{r}_2 \vec{r}_3 \vec{r}_4, \tau_1 \tau_2 \tau_3 \tau_4} = -\prod_{m=1}^{4} \left\{ \sum_{\vec{r}_m'} \left[(\mathcal{G}^c)^{-1}\right]^{a_m a_m'}_{\vec{r}_m \vec{r}_m', \tau_m \tau_m'} \right\} \mathcal{G}^{\overline{a_1' a_2' a_3' a_4'}, c}_{\vec{r}_1' \vec{r}_2' \vec{r}_3' \vec{r}_4', \tau_1' \tau_2' \tau_3' \tau_4'}. \tag{67}$$

In this work, we do not consider a trapping potential for simplicity. Therefore, local quantities such as n-point CCOGFs in the atomic limit have no spatial dependency, and henceforth we will drop the $\vec{r}$ index for these quantities.

3. Equations of motion

We now apply a 2PI [124] approach to our effective theory to obtain equations of motion for the mean-field and the full two-point CCOGF for the Φ-fields (the "full propagator" from now on). In a related work [92], we applied this approach to the homogeneous BHM in the strong coupling limit. We follow the same general procedure in this work with a few modifications to account for the additional vertices and auxiliary fields that appear in our effective theory of the disordered BHM as compared to that

of the homogeneous BHM. Here we only briefly outline the 2PI calculation. For a more detailed exposition of the 2PI approach, see Ref. [92].

We define the mean-field $\mathcal{V}^{\chi_1}$ and full propagator $\mathcal{V}^{\chi_1\chi_2,c}$ as follows

$$\mathcal{V}^{\chi_1} = \langle \Phi^{\chi_1} \rangle = \begin{pmatrix} \langle z^{a_1}_{r_1,\tau_1} \rangle \\ \left\langle \mathcal{Q}^{a_1' a_1''}_{r_1' r_1'',\tau_1' \tau_1''} \right\rangle \end{pmatrix}, \tag{68}$$

$$i\mathcal{V}^{\chi_1\chi_2,c} = \langle \Phi^{\chi_1}\Phi^{\chi_2} \rangle = \begin{pmatrix} \langle z^{a_1}_{r_1,\tau_1} z^{a_2}_{r_2,\tau_2} \rangle^c & \left\langle z^{a_1}_{r_1,\tau_1} \mathcal{Q}^{a_2' a_2''}_{r_2' r_2'',\tau_2' \tau_2''} \right\rangle^c \\ \left\langle \mathcal{Q}^{a_1' a_1''}_{r_1' r_1'',\tau_1' \tau_1''} \Psi^{a_2}_{r_2,\tau_2} \right\rangle^c & \left\langle \mathcal{Q}^{a_1' a_1''}_{r_1' r_1'',\tau_1' \tau_1''} \mathcal{Q}^{a_2' a_2''}_{r_2' r_2'',\tau_2' \tau_2''} \right\rangle^c \end{pmatrix}. \tag{69}$$

Next, we consider the 2PI Dyson's equation

$$\left[\mathcal{V}^{-1}\right]^{\chi_1\chi_2,c} = \left[D^{-1}\right]^{\chi_1\chi_2} - \left[\Sigma^{(2\mathrm{PI})}\right]^{\chi_1\chi_2}, \tag{70}$$

where

$$\begin{aligned} \left[D^{-1}\right]^{\chi_1\chi_2} &\equiv \frac{\delta^2 S\left[\mathcal{V}^{\chi}\right]}{\delta\mathcal{V}^{\chi_1}\delta\mathcal{V}^{\chi_2}} \\ &= \left[g_0^{-1}\right]^{\chi_1\chi_2} - \left[\Sigma^{(1)}\right]^{\chi_1\chi_2}. \end{aligned} \tag{71}$$

$\left[\Sigma^{(1)}\right]^{\chi_1\chi_2}$ is the "1-loop" self-energy

$$\left[\Sigma^{(1)}\right]^{\chi_1\chi_2} = -g^{\chi_1\chi_2} - g^{\chi_1\chi_2\chi_3}\mathcal{V}^{\chi_3} - \frac{1}{2}g^{\chi_1\chi_2\chi_3\chi_4}\mathcal{V}^{\chi_3}\mathcal{V}^{\chi_4}. \tag{72}$$

$\left[\Sigma^{(2\mathrm{PI})}\right]^{\chi_1\chi_2}$ is the 2PI self-energy

$$\left[\Sigma^{(2\mathrm{PI})}\right]^{\chi_1\chi_2} = 2i\frac{\delta\Gamma_2\left[\mathcal{V}^{\chi}, \mathcal{V}^{\chi\chi',c}\right]}{\delta\mathcal{V}^{\chi_1\chi_2,c}}, \tag{73}$$

and $\Gamma_2\left[\mathcal{V}^{(1)}, \mathcal{V}^{(2)}\right]$ is the sum of all 2PI connected vacuum diagrams in the theory with vertices determined by the action

$$\begin{aligned} S_{\mathrm{int}}\left[\Phi; \mathcal{V}^{(1)}\right] = &\frac{1}{3!}g^{\chi_1\chi_2\chi_3}\Phi^{\chi_1}\Phi^{\chi_2}\Phi^{\chi_3} \\ &+ \frac{1}{3!}g^{\chi_1\chi_2\chi_3\chi_4}\Phi^{\chi_1}\Phi^{\chi_2}\Phi^{\chi_3}\mathcal{V}^{\chi_4} \\ &+ \frac{1}{4!}g^{\chi_1\chi_2\chi_3\chi_4}\Phi^{\chi_1}\Phi^{\chi_2}\Phi^{\chi_3}\Phi^{\chi_4}. \end{aligned} \tag{74}$$

To first order in the vertices we have

$$\left[\Sigma^{(2\mathrm{PI})}\right]^{\chi_1\chi_2} = -\frac{i}{2}g^{\chi_1\chi_2\chi_3\chi_4}\mathcal{V}^{\chi_3\chi_4,c}. \tag{75}$$

If we define the full self-energy $\Sigma^{\chi_1\chi_2}$ to be

$$\Sigma^{\chi_1\chi_2} = \left[\Sigma^{(1)}\right]^{\chi_1\chi_2} + \left[\Sigma^{(2\mathrm{PI})}\right]^{\chi_1\chi_2}, \tag{76}$$

then we may rearrange the Dyson's equation as follows

$$\mathcal{V}^{\chi_1\chi_2,c} = \left[g_0\right]^{\chi_1\chi_2} + \left[g_0\right]^{\chi_1\chi_3}\Sigma^{\chi_3\chi_4}\mathcal{V}^{\chi_4\chi_2,c}. \tag{77}$$

Additionally, the equation of motion for the mean field $\mathcal{V}^{\chi_1}$ is

$$\frac{\delta S}{\delta\mathcal{V}^{\chi_1}} + \frac{i}{2}\left[\frac{\delta\left[D^{-1}\right]^{\chi_2\chi_3}}{\delta\mathcal{V}^{\chi_1}}\mathcal{V}^{\chi_2\chi_3,c}\right] = 0. \tag{78}$$

As will be clear shortly, we are mostly interested in finding $\mathcal{V}^{z_1}$ and $\mathcal{V}^{z_1 z_2,c}$, that can be calculated from Eqs. (78) and (77) respectively, for the equilibrium and out-of-equilibrium scenarios. First, we start with $\mathcal{V}^{z_1 z_2,c}$. From Dyson's equation (77) we can write

$$\mathcal{V}^{z_1 z_2,c} = \left[g_0\right]^{z_1 z_2} + \left[g_0\right]^{z_1 z_3}\Sigma^{z_3 z_4}\mathcal{V}^{z_4 z_2,c} + \left[g_0\right]^{z_1 z_3}\Sigma^{z_3 \mathcal{Q}_{45}}\mathcal{V}^{\mathcal{Q}_{45} z_2,c}, \tag{79}$$

where

$$\Sigma^{z_1 z_2} = -g^{z_1 z_2} - g^{z_1 z_2 \mathcal{Q}_{34}}\mathcal{V}^{\mathcal{Q}_{34}} - \frac{1}{2}g^{z_1 z_2 z_3 z_4}\mathcal{V}^{z_3}\mathcal{V}^{z_4} - \frac{i}{2}g^{z_1 z_2 z_3 z_4}\mathcal{V}^{z_3 z_4,c}, \tag{80}$$

$$\Sigma^{z_1 \mathcal{Q}_{23}} = -g^{z_1 \mathcal{Q}_{23} z_4}\mathcal{V}^{z_4}. \tag{81}$$

To make further progress, we cast Eq. (79) in terms of the correlation functions of the original a-fields. By inspection, one can see from Eq. (45) that $\mathcal{Z}[f, K]$ is the generator of COGFs of the z-fields in addition to the a-fields. This implies that

$$\mathcal{V}^{z_1} = \check{G}^{a_1}_{\vec{r}_1,\tau_1} \equiv \check{\phi}^{a_1}_{\vec{r}_1,\tau_1}, \tag{82}$$

$$\mathcal{V}^{z_1 z_2, c} = \check{G}^{a_1 a_2, c}_{\vec{r}_1 \vec{r}_2, \tau_1 \tau_2}, \tag{83}$$

where $\check{\phi}$ denotes the superfluid order parameter. Since we consider hopping strengths below the critical value of the Mott insulator to superfluid transition and assume that our initial state is of the form given in Eq. (43), we may safely assume that $\mathcal{V}^{z_1} = 0$. Note that this assumption is not valid when the system is in the superfluid phase as will be discussed in Sec. 3.2.2. For $\mathcal{V}^{\mathcal{Q}_{12}}$, we follow a similar calculation to that in Ref. [127]: using Eqs. (25) and (39) we can write

$$\begin{aligned}
\check{G}^{a_1 a_2, c}_{\vec{r}_1 \vec{r}_2, \tau_1 \tau_2} &= \check{G}^{a_1 a_2}_{\vec{r}_1 \vec{r}_2, \tau_1 \tau_2} \\
&= i \lim_{f \to 0} \frac{\delta^2 \check{\mathcal{Z}}[f]}{\delta f^{\overline{a_1}}_{\vec{r}_1,\tau_1} \delta f^{\overline{a_2}}_{\vec{r}_2,\tau_2}} \\
&= -2 \lim_{f \to 0} \int [\mathcal{D}a] \left\langle \mathbf{a}(\tau_i) \left| \hat{\rho}_i \right| \mathbf{a}(\tau_f) \right\rangle e^{-\frac{1}{2}\{\mathbf{a}(\tau_i).\mathbf{a}(\tau_i) + \mathbf{a}(\tau_f).\mathbf{a}(\tau_f)\}} \\
&\qquad \times \int [\mathcal{D}Q] e^{i\left(S_J[a] + S_0[a] + S_{M^{-1}}[Q]\right)} \left(\frac{\delta \left\{ e^{i(S_f[a] + S_Q[a])} \right\}}{Q^{\overline{a_1 a_2}}_{\vec{r}_1 \vec{r}_2, \tau_1 \tau_2}} \right),
\end{aligned} \tag{84}$$

then integrate by parts to get

$$\begin{aligned}
\check{G}^{a_1 a_2, c}_{\vec{r}_1 \vec{r}_2, \tau_1 \tau_2} &= 2 \lim_{f \to 0} \int [\mathcal{D}a] \left\langle \mathbf{a}(\tau_i) \left| \hat{\rho}_i \right| \mathbf{a}(\tau_f) \right\rangle e^{-\frac{1}{2}\{\mathbf{a}(\tau_i).\mathbf{a}(\tau_i) + \mathbf{a}(\tau_f).\mathbf{a}(\tau_f)\}} \\
&\qquad \times \int [\mathcal{D}Q] e^{i(S_J[a] + S_0[a] + S_f[a] + S_Q[a])} \left(\frac{\delta \left\{ e^{i\left(S_{M^{-1}}[Q]\right)} \right\}}{Q^{\overline{a_1 a_2}}_{\vec{r}_1 \vec{r}_2, \tau_1 \tau_2}} \right) \\
&= 2i \left[M^{-1} \right]^{[\![a_1 a_2]\!][\![a_3 a_4]\!]}_{[\![\tau_1 \tau_2]\!][\![\tau_3 \tau_4]\!]} \int [\mathcal{D}Q] \, Q^{\overline{a_3 a_4}}_{\vec{r}_3 \vec{r}_4, \tau_3 \tau_4} e^{i\bar{S}[Q]},
\end{aligned} \tag{85}$$

where

$$\begin{aligned}
e^{i\bar{S}[Q]} = \int [\mathcal{D}a] &\left\langle \mathbf{a}(\tau_i) \left| \hat{\rho}_i \right| \mathbf{a}(\tau_f) \right\rangle e^{-\frac{1}{2}\{\mathbf{a}(\tau_i).\mathbf{a}(\tau_i) + \mathbf{a}(\tau_f).\mathbf{a}(\tau_f)\}} \\
&\times e^{i\left(S_J[a] + S_0[a] + S_{M^{-1}}[Q] + S_f[a] + S_Q[a]\right)}.
\end{aligned} \tag{86}$$

Continuing with Eq. (85), we have

$$\begin{aligned}
\check{G}^{a_1 a_2, c}_{\vec{r}_1 \vec{r}_2, \tau_1 \tau_2} &= 2i \left[M^{-1} \right]^{[\![a_1 a_2]\!][\![a_3 a_4]\!]}_{[\![\tau_1 \tau_2]\!][\![\tau_3 \tau_4]\!]} \left\langle Q^{\overline{a_3 a_4}}_{\vec{r}_3 \vec{r}_4, \tau_3 \tau_4} \right\rangle \\
&= -\frac{2}{\widetilde{\Delta}^2_\epsilon} \left\langle Q^{\overline{a_1 a_2}}_{\vec{r}_1 \vec{r}_2, \tau_1 \tau_2} \right\rangle \\
&= -\frac{2}{\widetilde{\Delta}^2_\epsilon} \mathcal{V}^{\mathcal{Q}_{12}},
\end{aligned} \tag{87}$$

hence

$$\mathcal{V}^{\mathcal{Q}_{12}} = -\frac{1}{2} \widetilde{\Delta}^2_\epsilon \check{G}^{a_1 a_2, c}_{\vec{r}\vec{r}, \tau_1 \tau_2}. \tag{88}$$

Substituting Eqs. (53), (61)-(64), (82), (83), and (88) into Eq. (79) gives

$$\check{G}^{a_1 a_2, c}_{\vec{r}_1 \vec{r}_2, \tau_1 \tau_2} = \mathcal{G}^{a_1 a_2, c}_{\tau_1 \tau_2} + \mathcal{G}^{a_1 a_3, c}_{\tau_1 \tau_3} \left[\Sigma^{zz} \right]^{\overline{a_3 a_4}}_{\vec{r}_3 \vec{r}_4, \tau_3 \tau_4} \check{G}^{a_4 a_2, c}_{\vec{r}_4 \vec{r}_2, \tau_4 \tau_2}, \tag{89}$$

where

$$\left[\Sigma^{zz} \right]^{a_1 a_2}_{\vec{r}_1 \vec{r}_2, \tau_1 \tau_2} = \left[\Sigma^{zz}_1 \right]^{a_1 a_2}_{\vec{r}_1 \vec{r}_2, \tau_1 \tau_2} + \delta_{\vec{r}_1 \vec{r}_2} \left(\left[\Sigma^{zz}_2 \right]^{a_1 a_2}_{\vec{r}_1, \tau_1 \tau_2} + \left[\Sigma^{zz}_3 \right]^{a_1 a_2}_{\vec{r}_1, \tau_1 \tau_2} \right), \tag{90}$$

$$\left[\Sigma^{zz}_1 \right]^{a_1 a_2}_{\vec{r}_1 \vec{r}_2, \tau_1 \tau_2} = -2 J^{a_1 a_2}_{\vec{r}_1 \vec{r}_2, \tau_1 \tau_2}, \tag{91}$$

and the contributions to the self energy are

$$\left[\Sigma^{zz}_2 \right]^{a_1 a_2}_{\vec{r}, \tau_1 \tau_2} = -\tilde{u}^{a_1 a_2}_{\tau_1 \tau_2} - \frac{1}{2} u^{a_1 a_2 a_3 a_4}_{\tau_1 \tau_2 \tau_3 \tau_4} \left(i \check{G}^{\overline{a_3 a_4}, c}_{\vec{r}, \tau_3 \tau_4} \right), \tag{92}$$

and

$$\left[\Sigma_3^{zz}\right]^{a_1a_2}_{\vec{r},\tau_1\tau_2} = -\frac{i}{6}\widetilde{\Delta}_\epsilon^2 u^{a_1a_2[\![a_3a_4]\!]}_{\tau_1\tau_2[\![\tau_3\tau_4]\!]}\left(i\check{G}^{\overline{a_3a_4},c}_{\vec{r},\tau_3\tau_4}\right). \tag{93}$$

The next step is to calculate the mean field $\mathcal{V}^{z_1}$. Using Eqs. (51), (71) and (72) we can rewrite Eqs. (78) as

$$\begin{aligned}0 = &\left(2J^{z_1z_2} + \tilde{u}^{z_1z_2} + \left[(\mathcal{G}^c)^{-1}\right]^{z_1z_2}\right)\mathcal{V}^{z_2} \\ &+ g^{z_1z_2Q_{34}}\mathcal{V}^{z_2}\mathcal{V}^{Q_{34}} + \frac{1}{3!}g^{z_1z_2z_3z_4}\mathcal{V}^{z_2}\mathcal{V}^{z_3}\mathcal{V}^{z_4} \\ &+ ig^{z_1Q_{23}z_4}\mathcal{V}^{Q_{23}z_4,c} + \frac{i}{2}g^{z_1z_2z_3z_4}\mathcal{V}^{z_2}\mathcal{V}^{z_3z_4,c},\end{aligned} \tag{94}$$

where we used $\mathcal{V}^{Q_{12}z_3,c} = \mathcal{V}^{z_1Q_{23},c}$. Next we need to calculate $\mathcal{V}^{Q_{12}z_3,c}$. Using Eq. (77) again, we get

$$\mathcal{V}^{Q_{12}z_3,c} = \left[g_0\right]^{Q_{12}z_3} + \left[g_0\right]^{Q_{12}Q_{45}}\Sigma^{Q_{45}z_6}\mathcal{V}^{z_6z_3,c} + \left[g_0\right]^{Q_{12}Q_{45}}\Sigma^{Q_{45}Q_{67}}\mathcal{V}^{Q_{67}z_3,c}. \tag{95}$$

In order to make progress we treat the disorder strength perturbatively. Our results here are based on keeping terms to $\mathcal{O}\left(\widetilde{\Delta}_\epsilon^2\right)$. Since $\left[g_0\right]^{Q_{12}Q_{45}}$ is of order $\widetilde{\Delta}_\epsilon^2$, it forces the last term in Eq. (95) to be of order $\widetilde{\Delta}_\epsilon^4$. Therefore we approximate Eq. (95) by

$$\mathcal{V}^{Q_{12}z_3,c} = \left[g_0\right]^{Q_{12}Q_{45}}\Sigma^{Q_{45}z_6}\mathcal{V}^{z_6z_3,c} + \mathcal{O}\left(\widetilde{\Delta}_\epsilon^4\right), \tag{96}$$

where we also used the fact that $\left[g_0\right]^{Q_{12}z_3} = 0$. Now, using Eqs. (56), (61), (80), (81), (82), (83), (88) and (96) we can rewrite Eq. (94) as follows

$$\begin{aligned}0 = &\left(2J^{a_1a_2}_{\vec{r}_1\vec{r}_2\tau_1\tau_2} + \left[(\mathcal{G}^c)^{-1}\right]^{a_1a_2}_{\vec{r}_1\vec{r}_2,\tau_1\tau_2}\right)\check{\phi}^{\overline{a_2}}_{\vec{r}_2\tau_2} \\ &+ \frac{1}{3!}u^{a_1a_2a_3a_4}_{\tau_1\tau_2\tau_3\tau_4}\check{\phi}^{\overline{a_2}}_{\vec{r}_1\tau_2}\check{\phi}^{\overline{a_3}}_{\vec{r}_1\tau_3}\check{\phi}^{\overline{a_4}}_{\vec{r}_1\tau_4} + \frac{1}{2!}u^{a_1a_2a_3a_4}_{\tau_1\tau_2\tau_3\tau_4}\check{\phi}^{\overline{a_2}}_{\vec{r}_1\tau_2}\left(i\check{G}^{\overline{a_3a_4},c}_{\vec{r}_1\vec{r}_1,\tau_3\tau_4} - i\mathcal{G}^{\overline{a_3a_4},c}_{\vec{r}_1\vec{r}_1,\tau_3\tau_4}\right) \\ &- \frac{\widetilde{\Delta}_\epsilon^2}{9}u^{a_4a_1[\![a_2a_3]\!]}_{\tau_4\tau_1[\![\tau_2\tau_3]\!]}u^{\overline{[\![a_2a_3]\!]a_5a_6}}_{[\![\tau_2\tau_3]\!]\tau_5\tau_6}\check{\phi}^{\overline{a_6}}_{\vec{r}_1\tau_6}\check{G}^{\overline{a_5a_4},c}_{\vec{r}_1\vec{r}_1,\tau_5\tau_4} - \frac{\widetilde{\Delta}_\epsilon^2}{6}u^{a_1a_2[\![a_3a_4]\!]}_{\tau_1\tau_2[\![\tau_3\tau_4]\!]}\check{\phi}^{\overline{a_2}}_{\vec{r}_1\tau_2}\check{G}^{\overline{a_3a_4},c}_{\vec{r}_1\vec{r}_1,\tau_3\tau_4}.\end{aligned} \tag{97}$$

We will also be interested in calculating particle number to obtain the Mott insulator phase boundary, which can be calculated from G. To calculate G, we solve Eq. (89), however, the form shown here is still not particularly amenable to solution. We now discuss simplifications that allow us to obtain more tractable equations of motion.

3.1. Low-frequency approximation

Equation (89), whilst having a compact form in our notation, contains as many as four time-integrals, making it computationally expensive to solve the equations numerically. This suggests that some level of approximation beyond simply truncating the self-energy is required in order to obtain physical insight from the equations above. Following Refs. [91,92], we focus on the low-frequency components of the equations of motion, specifically the self-energy terms Σ_2^{zz} and Σ_3^{zz}.

$\Sigma_1^{zz} + \Sigma_2^{zz}$ is almost identical in form to the self-energy obtained in Ref. [93], the only difference being that the u-vertices have a trivial spatial dependency. Therefore the low-frequency calculation of Σ_2^{zz} is almost identical to that in Ref. [93] and can be written as

$$\left[\Sigma_2^{zz}\right]^{a_1a_2}_{\vec{r},\tau_1\tau_2} \simeq 2\delta\left(\tau_1,\tau_2\right)\sigma_1^{a_1a_2}u_1\left\{\check{n}_{\vec{r}}\left(\tau_1\right) - \check{n}_{\vec{r}}\left(\tau=0\right)\right\}, \tag{98}$$

where $\check{n}_{\vec{r}}(\tau)$ is the disorder-averaged particle number at site $\vec{r}$ and contour time τ, and u_1 comes from taking the low-frequency approximation of $u^{a_1a_2a_3a_4}_{\tau_1\tau_2\tau_3\tau_4}$, the expression for which is given in Appendix B. Provided μ/U is not close to an integer, then $u_1/U \ll 1$ [91,92]; and we also focus on the small $\widetilde{\Delta}_\epsilon^2$ limit, we keep terms of either order u_1 or $\widetilde{\Delta}_\epsilon^2$ but not terms of order $u_1\widetilde{\Delta}_\epsilon^2$ or higher.

Now, to calculate the low-frequency approximation to $\left[\Sigma_3^{zz}\right]^{a_1a_2}_{\vec{r},\tau_1\tau_2}$ it is helpful to rewrite $u^{a_1a_2[\![a_3a_4]\!]}_{\tau_1\tau_2[\![\tau_3\tau_4]\!]}$ as

$$\begin{aligned}u^{a_1a_2[\![a_3a_4]\!]}_{\tau_1\tau_2[\![\tau_3\tau_4]\!]} = &-i\frac{3}{2}\prod_{m=3}^{4}\left\{\mathcal{G}^{a_ma'_m,c}_{\tau_m\tau'_m}\right\}u^{a_1a_2\overline{a'_3a'_4}}_{\tau_1\tau_2\tau'_3\tau'_4} \\ &+ \frac{3}{2}\left\{\delta_{\tau_1\tau_3}\sigma_1^{a_1a_3}\right\}\left\{\delta_{\tau_2\tau_4}\sigma_1^{a_2a_4}\right\} + \frac{3}{2}\left\{\delta_{\tau_1\tau_4}\sigma_1^{a_1a_4}\right\}\left\{\delta_{\tau_2\tau_3}\sigma_1^{a_2a_3}\right\}.\end{aligned} \tag{99}$$

By casting $u^{a_1a_2[\![a_3a_4]\!]}_{\tau_1\tau_2[\![\tau_3\tau_4]\!]}$ in this form, one can then perform a similar calculation to that for Σ_2^{zz} to obtain

$$\left[\Sigma_3^{zz}\right]^{a_1a_2,(R,A,K)}_{\vec{r}}\left(\tau_1,\tau_2\right) \simeq -\frac{i}{2}\widetilde{\Delta}_\epsilon^2\left\{i\check{G}^{a_1a_2,(R,A,K)}_{\vec{r}}\left(\tau_1,\tau_2\right)\right\}. \tag{100}$$

After applying the low-frequency approximation, we obtain a self-energy that is identical in Keldysh structure to the low-frequency self-energy obtained in Ref. [93] (for a discussion about Keldysh structure, see Ref. [92]). Therefore the equations of motion of the full propagator for the disordered system are identical in structure to those obtained in Ref. [93]. With this in mind, it is straightforward to show that the equations of motion can be written as follows:

$$\check{G}^{(R,A)}_{\vec{r}\vec{r}'}(t_1,t_2) = \mathcal{G}^{(R,A)}_{\vec{r}}(t_1,t_2) + \sum_{\vec{r}}\int_0^\infty\int_0^\infty dt_3 dt_4\, \mathcal{G}^{(R,A)}_{\vec{r}}(t_1,t_3)\left[\Sigma^{zz}\right]^{(R,A)}_{\vec{r}\vec{r}''}(t_3,t_4)\,\check{G}^{(R,A)}_{\vec{r}''\vec{r}'}(t_4,t_2), \tag{101}$$

$$\begin{aligned}\check{G}^{(K)}_{\vec{r}\vec{r}'}(t_1,t_2) = {}& \mathcal{G}^{(K)}_{\vec{r}}(t_1,t_2) + \sum_{\vec{r}}\int_0^\infty\int_0^\infty dt_3 dt_4\, \mathcal{G}^{(R)}_{\vec{r}}(t_1,t_3)\left[\Sigma^{zz}\right]^{(R)}_{\vec{r}\vec{r}''}(t_3,t_4)\,\check{G}^{(K)}_{\vec{r}''\vec{r}'}(t_4,t_2)\\ &+ \sum_{\vec{r}}\int_0^\infty\int_0^\infty dt_3 dt_4\, \mathcal{G}^{(K)}_{\vec{r}}(t_1,t_3)\left[\Sigma^{zz}\right]^{(A)}_{\vec{r}\vec{r}''}(t_3,t_4)\,\check{G}^{(A)}_{\vec{r}''\vec{r}'}(t_4,t_2),\end{aligned} \tag{102}$$

where $\check{G}^{(R)}_{\vec{r}\vec{r}'}(t,t')$ and $\check{G}^{(A)}_{\vec{r}\vec{r}'}(t,t')$ are the disorder averaged full retarded and advanced Green's functions respectively obtained from performing a disorder average (as in Eq. (24)) of the quantities

$$G^{(R)}_{\vec{r}\vec{r}'}(t,t';\epsilon) = -i\Theta(t-t')\left\langle a_{\vec{r}}(t;\epsilon)\, a^\dagger_{\vec{r}'}(t';\epsilon) - a^\dagger_{\vec{r}'}(t';\epsilon)\, a_{\vec{r}}(t;\epsilon)\right\rangle_S, \tag{103}$$

$$G^{(A)}_{\vec{r}\vec{r}'}(t,t';\epsilon) = i\Theta(t'-t)\left\langle a_{\vec{r}}(t;\epsilon)\, a^\dagger_{\vec{r}'}(t';\epsilon) - a^\dagger_{\vec{r}'}(t';\epsilon)\, a_{\vec{r}}(t;\epsilon)\right\rangle_S, \tag{104}$$

and $\check{G}^{(K)}_{\vec{r}}(t,t')$ is the disorder averaged full kinetic Green's function obtained from disorder averaging

$$G^{(K)}_{\vec{r}\vec{r}'}(t,t';\epsilon) = -i\left\langle a_{\vec{r}}(t;\epsilon)\, a^\dagger_{\vec{r}'}(t';\epsilon) + a^\dagger_{\vec{r}'}(t';\epsilon)\, a_{\vec{r}}(t;\epsilon)\right\rangle_S. \tag{105}$$

The quantities $\mathcal{G}^{(R)}_{\vec{r}}(t-t')$, $\mathcal{G}^{(A)}_{\vec{r}}(t-t')$, and $\mathcal{G}^{(K)}_{\vec{r}}(t-t')$ that enter Eqs. (101) and (102) are the W_0-generated retarded, advanced and kinetic Green's functions, respectively, which are all time-translational invariant (expressions for each are presented in Appendix A). It is important to note that $\check{n}_{\vec{r}}(t)$ can be obtained from $\check{G}^{(K)}_{\vec{r}\vec{r}'}(t,t')$ as follows:

$$\check{n}_{\vec{r}}(t) = \frac{1}{2}\left\{i\check{G}^{(K)}_{\vec{r}\vec{r}}(t,t) - 1\right\}, \tag{106}$$

which introduces an element of nonlinearity into the equations of motion above.

Finally, in the low-frequency limit, we can approximate Eq. (97) as

$$\begin{aligned}0 = {}& 2\sum_{\vec{r}'} J_{\vec{r}\vec{r}'}(t_1)\,\check{\phi}_{\vec{r}'}(t_1) + \left[(\mathcal{G}^c)^{-1}\right]^{(R)}_{\omega\to 0}\check{\phi}_{\vec{r}}(t_1) - 2u_1\check{\phi}_{\vec{r}}(t_1)\left[\check{n}_{\vec{r}}(t_1) - \check{n}_{\vec{r}}(t_1'=0)\right]\\ &- u_1\check{\phi}_{\vec{r}}(t_1)\left|\check{\phi}_{\vec{r}}(t_1)\right|^2 - \widetilde{\Delta}^2_\epsilon\check{\phi}_{\vec{r}}(t_1)\,\check{G}^{12,(R)}_{\vec{r}\vec{r}}(t_1,t_2),\end{aligned} \tag{107}$$

where $\left[(\mathcal{G}^c)^{-1}\right]^{(R)}_{\omega\to 0}$ is the low-frequency approximation of the inverse retarded Green's function obtained from W_0, the expression for which is given in Appendix B.

3.2. Equilibrium solution

In studying the equilibrium solution to the equations of motion derived in Sec. 3.1 we consider the system to be at zero temperature. We also work in $\vec{k}$-space rather than real space. Whilst disordered systems are not homogeneous due to the random potential in the Hamiltonian, the disorder-averaged COGFs respect translation invariance. Therefore we follow the same procedure as Ref. [92] in order to obtain the Mott insulator phase boundary in the presence of disorder. The only difference being that now the COGFs are replaced by disorder-averaged COGFs. In $\vec{k}$-space Eq. (89) becomes

$$\check{G}^{a_1a_2,(R)}_{\vec{k}}(\omega) = \mathcal{G}^{a_1a_2,(R)}(\omega) + \mathcal{G}^{a_1a_3,(R)}(\omega)\left[\Sigma^{zz}\right]^{\overline{a_3a_4},(R)}_{\vec{k}}(\omega)\,\check{G}^{a_4a_2,(R)}_{\vec{k}}(\omega), \tag{108}$$

where $[\Sigma^{zz}]^{\overline{a_3a_4},(R)}_{\vec{k}}(\omega)$ is the Fourier transform of $[\Sigma^{zz}]^{a_1a_2}_{\vec{r}_1\vec{r}_2,\tau_1\tau_2}$. Now we can write

$$\left[\Sigma^{zz}\right]^{12,(R)}_{\vec{k}}(\omega) = -2J\sum_{i=1}^d\cos(k_ia) + 2u_1\left[\left|\check{\phi}\right|^2 + (\check{n}-\check{n}_0)\right] + \frac{1}{2}\widetilde{\Delta}^2_\epsilon\check{G}^{12,(R)}_{\vec{k}}(\omega) + \mathcal{O}\left(u_1\widetilde{\Delta}^2_\epsilon\right), \tag{109}$$

$$\left[\Sigma^{zz}\right]^{11,(R)}_{\vec{k}}(\omega) = \frac{1}{2}u_1\left[2\left(\check{\phi}^1\right)^2 + i\check{G}^{11,(K)}_{\vec{r}'=0}(s=0)\right] + \frac{1}{2}\widetilde{\Delta}^2_\epsilon\check{G}^{11,(R)}_{\vec{k}}(\omega), \tag{110}$$

$$\left[\Sigma^{zz}\right]^{22,(R)}_{\vec{k}}(\omega) = \frac{1}{2}u_1\left[2\left(\check{\phi}^2\right)^2 + i\check{G}^{22,(K)}_{\vec{r}'=0}(s=0)\right] + \frac{1}{2}\widetilde{\Delta}^2_\epsilon\check{G}^{22,(R)}_{\vec{k}}(\omega), \tag{111}$$

where $\check{n}$ is the average local particle number for $J\neq 0$

$$\check{n} = \left\langle\check{n}_{\vec{k}}\right\rangle = \frac{1}{N_{\text{site}}}\sum_{\vec{k}}\check{n}_{\vec{k}}. \tag{112}$$

Now, from Eq. (108) we can write

$$\check{G}^{12,(R)}_{\vec{k}}(\omega)=\frac{\left[\left\{\mathcal{G}^{21,(R)}(\omega)\right\}^{-1}-[\Sigma^{zz}]^{21,(R)}_{\vec{k}}(\omega)\right]}{\left[\left\{\mathcal{G}^{21,(R)}(\omega)\right\}^{-1}-[\Sigma^{zz}]^{21,(R)}_{\vec{k}}(\omega)\right]\left[\left\{\mathcal{G}^{12,(R)}(\omega)\right\}^{-1}-[\Sigma^{zz}]^{12,(R)}_{\vec{k}}(\omega)\right]-\left|[\Sigma^{zz}]^{22,(R)}_{\vec{k}}(\omega)\right|^2}, \tag{113}$$

$$\check{G}^{22,(R)}_{\vec{k}}(\omega)=\frac{[\Sigma^{zz}]^{22,(R)}_{\vec{k}}(\omega)}{\left[\left\{\mathcal{G}^{21,(R)}(\omega)\right\}^{-1}-[\Sigma^{zz}]^{21,(R)}_{\vec{k}}(\omega)\right]\left[\left\{\mathcal{G}^{12,(R)}(\omega)\right\}^{-1}-[\Sigma^{zz}]^{12,(R)}_{\vec{k}}(\omega)\right]-\left|[\Sigma^{zz}]^{22,(R)}_{\vec{k}}(\omega)\right|^2}. \tag{114}$$

In the following, we will discuss equilibrium solutions for the Mott insulator and superfluid phases. For simplicity we only consider the static limit, i.e., $\omega=0$. As we demonstrate later, this assumption is acceptable at least in equilibrium.

3.2.1. Mott insulator

In the Mott insulator phase $\check{\phi}$ and $[\Sigma^{zz}]^{22,(R)}_{\vec{k}}(\omega)$ are zero and $[\Sigma^{zz}]^{12,(R)}_{\vec{k}}(\omega)$ is

$$\left[\Sigma^{zz}\right]^{12,(R)}_{\vec{k}}=-2J\sum_{i=1}^{d}\cos(\vec{k}_i a)+2u_1\left(\check{n}-\check{n}_0\right)+\frac{1}{2}\tilde{\Delta}^2_{\epsilon}\check{G}^{12,(R)}_{\vec{k}}(\omega=0). \tag{115}$$

Therefore Eq. (113) reduces to

$$\check{G}^{12,(R)}_{\vec{k}}(\omega)=\frac{1}{\left[\left\{\mathcal{G}^{(R)}(\omega)\right\}^{-1}-[\Sigma^{zz}]^{12,(R)}_{\vec{k}}\right]}, \tag{116}$$

which we can rewrite as [92]

$$\check{G}^{12,(R)}_{\vec{k}}(\omega)=\tilde{z}^{(+)}_{\mathrm{MI},\vec{k}}\frac{1}{\left\{\omega-\Delta\tilde{E}^{(+)}_{\mathrm{MI},\vec{k}}\right\}+i0^+}-\tilde{z}^{(-)}_{\mathrm{MI},\vec{k}}\frac{1}{\left\{\omega+\Delta\tilde{E}^{(-)}_{\mathrm{MI},\vec{k}}\right\}+i0^+}, \tag{117}$$

where

$$\Delta\tilde{E}^{(\pm)}_{\mathrm{MI},\vec{k}}=\frac{\mp B_{\vec{k}}+\sqrt{\left(B_{\vec{k}}\right)^2-4C_{\vec{k}}}}{2}, \tag{118}$$

$$B_{\vec{k}}=-\left\{\Delta\mathcal{E}^{(+)}-\Delta\mathcal{E}^{(-)}\right\}-\Sigma^{12,(R)}_{\vec{k}}, \tag{119}$$

$$C_{\vec{k}}=-(\mu+U)\left[\Sigma^{12,(R)}_{\vec{k}}-\left\{\mathcal{G}^{(R)}\left(\omega'=0\right)\right\}^{-1}\right], \tag{120}$$

$$\tilde{z}^{(\pm)}_{\mathrm{MI},\vec{k}}=\frac{(\mu+U)\pm\Delta\tilde{E}^{(\pm)}_{\mathrm{MI},\vec{k}}}{\Delta\tilde{E}^{(+)}_{\mathrm{MI},\vec{k}}+\Delta\tilde{E}^{(-)}_{\mathrm{MI},\vec{k}}}, \tag{121}$$

and $\Delta\mathcal{E}^{(\pm)}$ are the excitation energies in the atomic limit (i.e. $J=0$)

$$\Delta\mathcal{E}^{(+)}=\mathcal{E}_{n_{\mathrm{MI}}+1}-\mathcal{E}_{n_{\mathrm{MI}}}, \tag{122}$$

$$\Delta\mathcal{E}^{(-)}=\mathcal{E}_{n_{\mathrm{MI}}-1}-\mathcal{E}_{n_{\mathrm{MI}}}. \tag{123}$$

As explained in Ref. [92], the local particle number can be expressed as

$$\check{n}_{\vec{k}}=\frac{1}{2}\left\{\tilde{z}^{(+)}_{\mathrm{MI},\vec{k}}+\tilde{z}^{(-)}_{\mathrm{MI},\vec{k}}-1\right\}. \tag{124}$$

In Fig. 2 we show the excitation energies $\Delta\tilde{E}^{(\pm)}_{\mathrm{MI},\vec{k}}$, and the spectral weights $\tilde{z}^{(\pm)}_{\mathrm{MI},\vec{k}}$ for different disorder strengths Δ_ϵ in the Mott insulator phase where the relation between Δ_ϵ and $\tilde{\Delta}_\epsilon$ is given in Eq. (30) and from now on we drop the ϵ index in Δ_ϵ to avoid confusion. In addition, we compare the quasi-momentum distribution $\check{n}_{\vec{k}}$ for two different disorder strengths: $\Delta/U=0.1$ and $\Delta/U=0.3$. Here we have a 1000×1000 square lattice, the chemical potential is $\mu/U=0.42$, the hopping strength is chosen to be $J/U=0.02$, and $\beta U=\infty$. As can be seen from Fig. 2, in the Mott phase, the excitation energies decrease with increasing disorder strength. In addition, with increasing disorder strength, the quasi-momentum distribution $\check{n}_{\vec{k}}$ becomes more localized, which implies that for the same hopping term, the system is closer to the transition point.

3.2.2. Superfluid

In the superfluid phase, $\check{\phi}$ and $[\Sigma^{zz}]^{22,(R)}_{\vec{k}}$ are non-zero, hence we must use the full forms of Eqs. (113) and (114). We begin by calculating $\check{\phi}$ from Eq. (107). Note that in writing Eq. (107), in order to obtain a gapless energy spectrum, we used the HFB-Popov [128] (HFBP) approximation as explained in detail in Ref. [92]. Here, we extend the HFB-Popov approximation to the disordered case (see Appendix C). Therefore we have

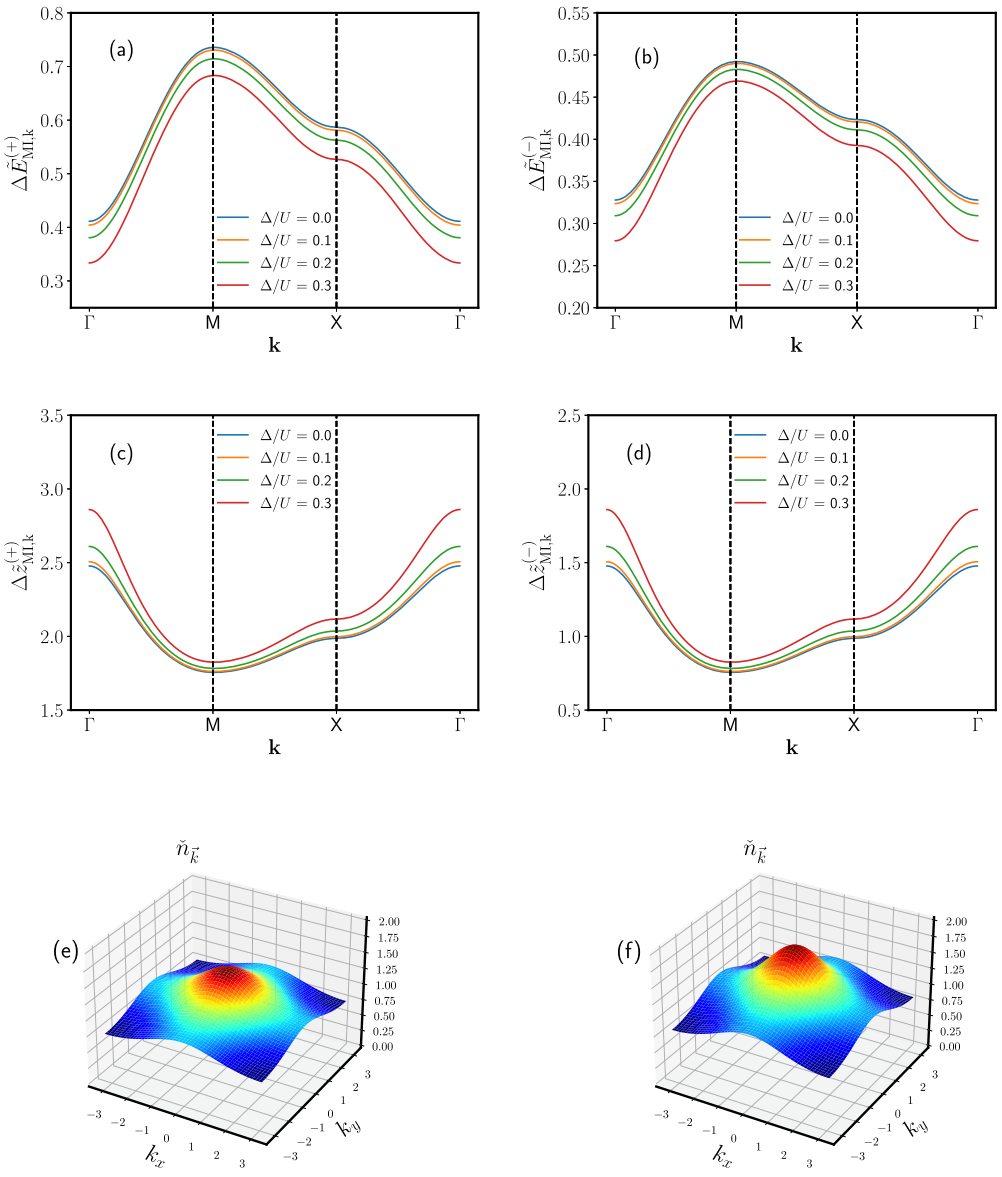

Fig. 2. Collective excitations of the Mott phase of the 2-dimensional disordered-BHM (a) Quasi-particle excitation energies $\Delta\tilde{E}^{(+)}_{\mathrm{MI},\vec{k}}$, (b) Quasi-hole excitation energies $\Delta\tilde{E}^{(-)}_{\mathrm{MI},\vec{k}}$, (c) Quasi-particle spectral weights $\tilde{z}^{(+)}_{\mathrm{MI},\vec{k}}$, (d) Quasi-hole spectral weights $\tilde{z}^{(-)}_{\mathrm{MI},\vec{k}}$, for different disorder strengths. Panels (e) and (f) show quasi-momentum distribution $\check{n}_{\vec{k}}$ for $\Delta/U = 0.1$, and $\Delta/U = 0.3$ respectively. The parameters used were $N_s = 1000^2$, $\mu/U = 0.42$, $J/U = 0.02$, and $\beta U = \infty$. Note that $\Gamma = (0,0)$, $M = (\pi,\pi)$, and $X = (\pi,0)$.

$$\check{\phi} = \sqrt{\frac{\left\{\mathcal{G}^{(R)}(\omega'=0)\right\}^{-1} + 2dJ - \tilde{\Delta}_\epsilon^2\left\{\check{G}^{12,(R)}_{\vec{k}}(\omega=0)\right\}}{u_1}} - 2\left(\check{n}-\check{n}_0\right) - \frac{i}{2}\check{G}^{22,(K)}_{\vec{r}'=0}(s=0)\,, \tag{125}$$

where

$$\check{G}^{22,(K)}_{\vec{r}'=0}(s=0) = \frac{i\tilde{\Delta}_\epsilon^2}{2u_1}\left[\check{G}^{12,(R)}_{\vec{k}=0}(\omega=0) + \check{G}^{22,(R)}_{\vec{k}=0}(\omega=0)\right]. \tag{126}$$

Now, in the superfluid phase, using Eqs. (109), (110), (111) and (125) we have that the self-energy is

$$\left[\Sigma^{zz}\right]^{12,(R)}_{\vec{k}}(\omega) = -2J\sum_{i=1}^{d}\cos(k_i a) + 2u_1\left[\left|\check{\phi}\right|^2 + \left(\check{n}-\check{n}_0\right)\right] + \frac{1}{2}\tilde{\Delta}_\epsilon^2\check{G}^{12,(R)}_{\vec{k}}(\omega=0)\,, \tag{127}$$

$$\left[\Sigma^{zz}\right]^{11,(R)}_{\vec{k}}(\omega) = u_1\check{\phi}^2 + \frac{1}{2}\tilde{\Delta}_\epsilon^2\check{G}^{11,(R)}_{\vec{k}}(\omega) - \frac{\tilde{\Delta}_\epsilon^2}{4}\left(\check{G}^{12,(R)}_{\vec{k}=0}(\omega=0) + \check{G}^{11,(R)}_{\vec{k}=0}(\omega=0)\right), \tag{128}$$

and

$$\left[\Sigma^{zz}\right]^{22,(R)}_{\vec{k}}(\omega) = u_1\check{\phi}^2 + \frac{1}{2}\widetilde{\Delta}^2_{\epsilon}\check{G}^{22,(R)}_{\vec{k}}(\omega) - \frac{\widetilde{\Delta}^2_{\epsilon}}{4}\left(\check{G}^{12,(R)}_{\vec{k}=0}(\omega=0) + \check{G}^{22,(R)}_{\vec{k}=0}(\omega=0)\right). \tag{129}$$

Next, we calculate $\check{G}^{(R)}$: starting from Eq. (114), one can show that

$$\check{G}^{12,(R)}_{\vec{k}}(\omega) = \frac{\left\{\omega^+ + \Delta\tilde{E}^{(+)}_{\mathrm{MI},\vec{k}}\right\}\left\{\omega^+ - \Delta\tilde{E}^{(-)}_{\mathrm{MI},\vec{k}}\right\}\left\{\omega^+ + (\mu+U)\right\}}{\left\{\omega^+ - \Delta\tilde{E}^{(1)}_{SF,\vec{k}}\right\}\left\{\omega^+ + \Delta\tilde{E}^{(1)}_{\mathrm{SF},\vec{k}}\right\}\left\{\omega^+ - \Delta\tilde{E}^{(2)}_{\mathrm{SF},\vec{k}}\right\}\left\{\omega^+ + \Delta\tilde{E}^{(2)}_{\mathrm{SF},\vec{k}}\right\}}, \tag{130}$$

where

$$\Delta\tilde{E}^{(s)}_{\mathrm{SF},\vec{k}} = \sqrt{\frac{-\tilde{B}_{\vec{k}} - (-1)^s\sqrt{\left(\tilde{B}_{\vec{k}}\right)^2 - 4\tilde{C}_{\vec{k}}}}{2}}, \tag{131}$$

$$\tilde{B}_{\vec{k}} = \left|\left[\Sigma^{zz}\right]^{22,(R)}_{\vec{k}}\right|^2 - \left\{\Delta\tilde{E}^{(+)}_{\mathrm{MI},\vec{k}}\right\}^2 - \left\{\Delta\tilde{E}^{(-)}_{\mathrm{MI},\vec{k}}\right\}^2, \tag{132}$$

and

$$\tilde{C}_{\vec{k}} = \left\{\Delta\tilde{E}^{(+)}_{\mathrm{MI},\vec{k}}\Delta\tilde{E}^{(-)}_{\mathrm{MI},\vec{k}}\right\}^2 - (\mu+U)\left|\left[\Sigma^{zz}\right]^{22,(R)}_{\vec{k}}\right|^2. \tag{133}$$

It is important to note that the expressions for B and C differ from those for the Mott insulator in that B has units of *energy* for the MI but units of $\left[energy\right]^2$ for the SF. Following the same approach as Ref. [92], the quasi-momentum $\check{n}_{\vec{k}}$ for $\vec{k}\neq 0$ is

$$\check{n}_{\vec{k}} = \begin{cases} \frac{1}{2}\left\{\tilde{z}^{(1,+)}_{\mathrm{SF},\vec{k}} + \tilde{z}^{(1,-)}_{\mathrm{SF},\vec{k}} + \tilde{z}^{(2,+)}_{\mathrm{SF},\vec{k}} + \tilde{z}^{(2,-)}_{\mathrm{SF},\vec{k}} - 1\right\}, & \text{if } \vec{k}\neq 0 \\ \frac{1}{2}\left\{\tilde{z}^{(1,+)}_{\mathrm{SF},\vec{k}} + \tilde{z}^{(1,-)}_{\mathrm{SF},\vec{k}} + 2N_{sites}\left|\check{\phi}\right|^2 - 1\right\}, & \text{if } \vec{k}=0 \end{cases}, \tag{134}$$

where

$$\tilde{z}^{(s,\pm)}_{\mathrm{SF},\vec{k}} = (-1)^{s+1}\frac{\left\{\Delta\tilde{E}^{(s)}_{\mathrm{SF},\vec{k}} \pm \Delta\tilde{E}^{(+)}_{\mathrm{MI},\vec{k}}\right\}\left\{\Delta\tilde{E}^{(s)}_{\mathrm{SF},\vec{k}} \mp \Delta\tilde{E}^{(-)}_{\mathrm{MI},\vec{k}}\right\}\left\{(\mu+U) \pm \Delta\tilde{E}^{(s)}_{\mathrm{SF},\vec{k}}\right\}}{2\Delta\tilde{E}^{(s)}_{\mathrm{SF},\vec{k}}\left[\left\{\Delta\tilde{E}^{(1)}_{\mathrm{SF},\vec{k}}\right\}^2 + \left\{\Delta\tilde{E}^{(2)}_{\mathrm{SF},\vec{k}}\right\}^2\right]}. \tag{135}$$

In Fig. 3 we show the collective mode spectra and quasi-particle spectral weight in the superfluid phase for different disorder strengths as calculated from Eqs. (131) and (135). To perform the numerical calculations we used a 1000×1000 square lattice, and set the chemical potential $\mu/U = 0.36$, the hopping to $J/U = 0.03$, and $\beta U = \infty$.

3.2.3. Mott insulator phase boundary

To obtain the Mott Insulator – Bose Glass (MI-BG) phase boundary, we calculate the critical hopping J_c at which $\check{\phi}=0$. This can be done numerically using Eq. (125). In Fig. 4 we show the phase boundary for different disorder strengths for dimensions one, two, and three.

In Refs. [112,113], the MI-BG transition for the chemical potential at the tip of the Mott lobe was calculated for two and three dimensional cubic lattices with random disorder uniformly distributed on the interval $[-\Delta,\Delta]$. In Fig. 5, using the disordered BHM in the strong coupling regime, we calculated the MI-BG transition and compared our results keeping terms to $\mathcal{O}\left(\widetilde{\Delta}^2_{\epsilon}\right)$ with those obtained using QMC simulations [112,113]. We find good agreement between our results and QMC simulations. It should be noted that we consider a Gaussian distribution of disorder, while Refs. [112,113] used a box distribution.

Finally, we consider the same set of parameters reported in Ref. [61] in which thermalization-MBL transition occurs. As is demonstrated in Fig. 6 we note that the reported critical point in Ref. [61] sits on top of the QMC determined phase transition.

4. Discussion and conclusions

In this work, we extended the 2PISC approach to the BHM to include the effects of disorder. We obtained a disorder-averaged effective theory from which we obtained the 2PI equations of motion for the superfluid order parameter and two, three and four-point correlations. These equations apply both in and out of equilibrium. A strength of the 2PISC is that it is applicable in one, two, and three spatial dimensions. This is particularly advantageous for out-of-equilibrium dynamics, where numerical methods that are essentially exact, such as exact diagonalization or DMRG, are limited to one dimension or very small system sizes.

A weakness of the 2PISC method is that in order to make progress, one needs to truncate the effective action, which was done at quartic order, and this is an uncontrolled approximation. However, previous results in the clean case for both the phase boundary in equilibrium [92] and agreement with exact diagonalization for out-of-equilibrium dynamics [93] give confidence in its usefulness. It should be noted that the accuracy appears to be greatest for larger U/J [96]. The main result of this paper is the derivation of

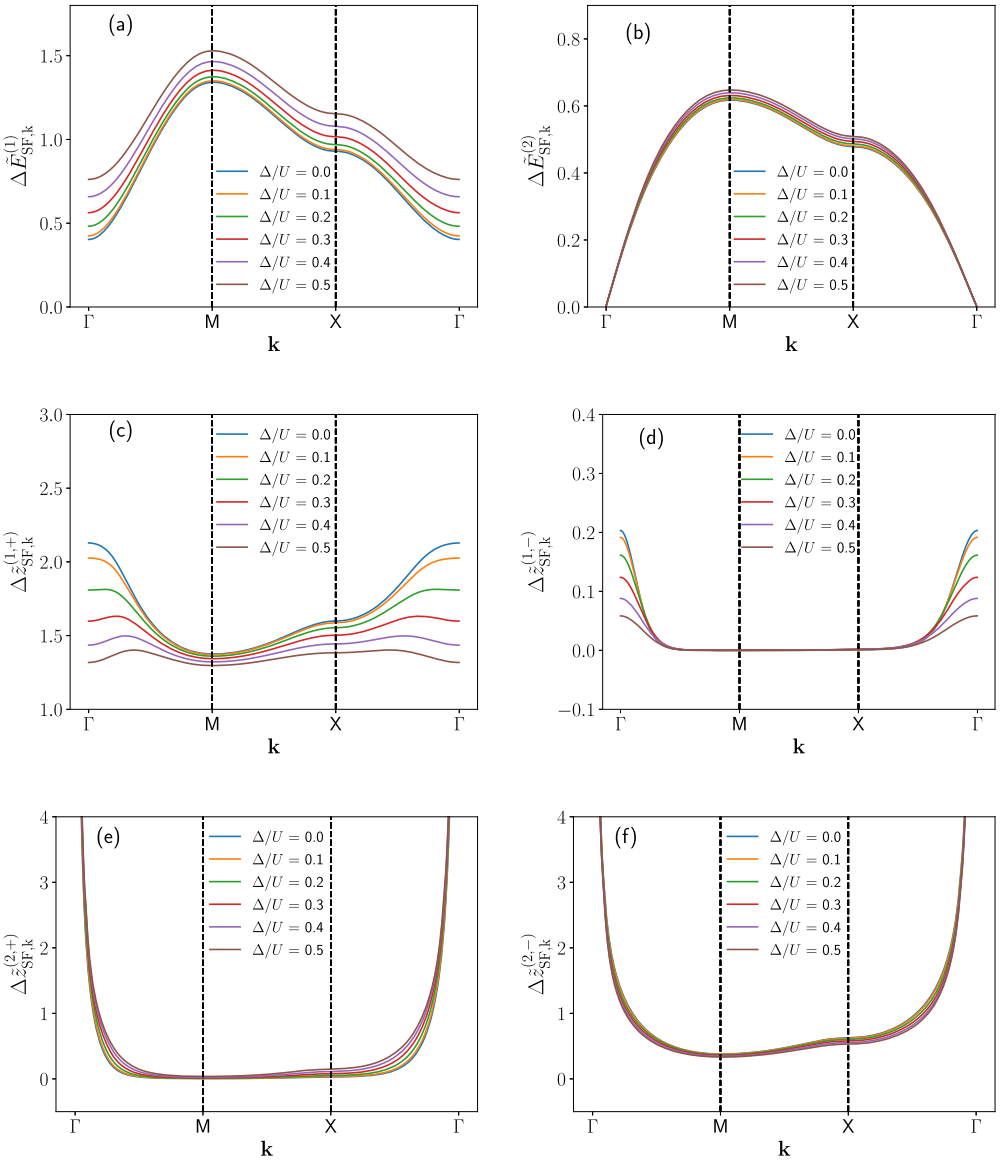

Fig. 3. Collective excitations for the superfluid phase of the two-dimensional disordered-BHM (a) first quasi-particle/hole excitation energy branch $\Delta\tilde{E}^{(1)}_{\mathrm{SF},\vec{k}}$, (b) second quasi-particle/hole excitation energy branch $\Delta\tilde{E}^{(2)}_{\mathrm{SF},\vec{k}}$, (c) quasi-particle spectral weights $\tilde{z}^{(1,+)}_{\mathrm{SF},\vec{k}}$ for the first branch, (d) quasi-hole spectral weights $\tilde{z}^{(1,-)}_{\mathrm{SF},\vec{k}}$ for the first branch, (e) quasi-particle spectral weights $\tilde{z}^{(2,+)}_{\mathrm{SF},\vec{k}}$ for the second branch, (f) quasi-hole spectral weights $\tilde{z}^{(2,-)}_{\mathrm{SF},\vec{k}}$ for the second branch for different disorder strengths. The parameters used were $N_s = 1000^2$, $\mu/U = 0.36$, $J/U = 0.07$, and $\beta U = \infty$. Note that $\Gamma = (0,0)$, $M = (\pi,\pi)$, and $X = (\pi,0)$.

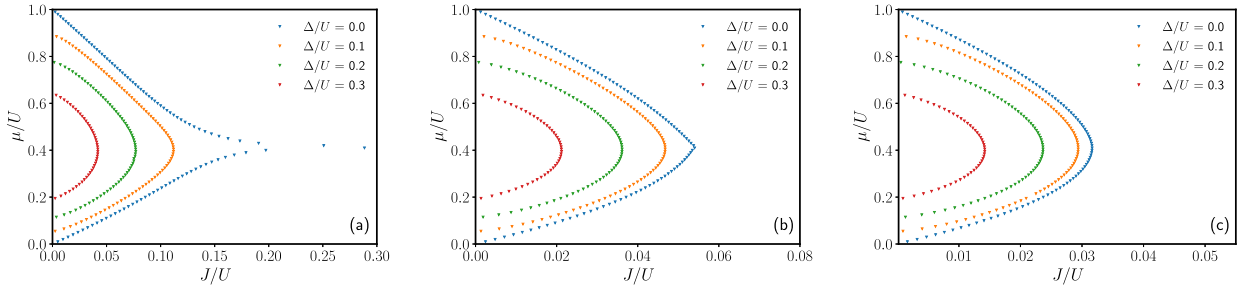

Fig. 4. Mott insulator phase boundaries for different disorder strengths for (a) d = 1, (b) d = 2, and (c) d = 3. Calculations performed keeping disorder terms to $\mathcal{O}\left(\widetilde{\Delta}^2_\epsilon\right)$.

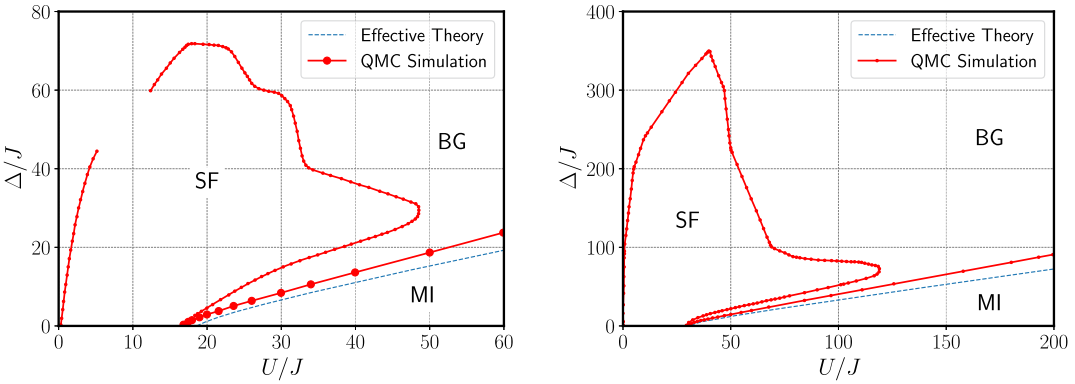

Fig. 5. Comparison of the results from effective theory to $\mathcal{O}\left(\tilde{\Delta}_\epsilon^2\right)$ and QMC for the Mott insulator – Bose glass transition for (a) $d = 2$ and (b) $d = 3$. QMC data for both the Mott insulator – Bose glass and Bose glass – superfluid transition taken for $d = 2$ from Ref. [112] and for $d = 3$ from Ref. [113].

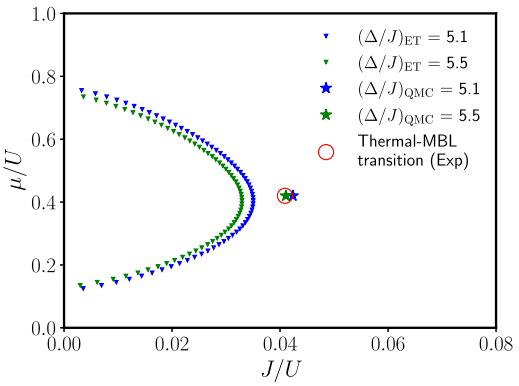

Fig. 6. Comparison of the experimentally identified thermal-MBL transition point (Red circle) at $U/J = 24.4$ for unit filling with the Mott insulator – Bose glass transition curves for $\Delta/J = 5.1$ and $\Delta/J = 5.5$ (corresponding to $\Delta/J = 5.3(2)$) obtained using the effective theory to $\mathcal{O}\left(\tilde{\Delta}_\epsilon^2\right)$. Blue and green stars are the corresponding QMC Mott insulator – Bose glass transition points for $\Delta/J = 5.1$ and $\Delta/J = 5.5$, respectively taken from Ref. [112].

the effective theory and the 2PI equations of motion, but as a check on the theory, we solved the disorder-averaged equations of motion in the equilibrium limit. We obtained the collective excitation spectra for the disordered BHM in both the Mott and superfluid phases and also obtained the Mott insulator phase boundary at a variety of disorder strengths in one, two, and three dimensions. We compared our results with QMC simulations performed for two and three dimensions in Refs. [112,113] and found very good agreement with the exact phase boundary.

Previous comparison of Mott insulator phase boundaries with QMC calculations in the clean case [92] found the 2PISC method gave a big improvement over the mean-field theory but was not in complete quantitative agreement with QMC calculation. We find a similar situation in the disordered case. However, there are caveats, in that we consider a Gaussian distribution of disorder rather than the box distribution used in Refs. [112] and [113]. We also treat the disorder perturbatively and keep the highest-order term only (calculations to order $\tilde{\Delta}_\epsilon^2$). Given that there are uncontrolled approximations in the 2PISC method, these results give confidence in the results here and future applications to the out-of-equilibrium dynamics of the disordered Bose-Hubbard model. One limitation of our method is that we have not been able to determine the Bose glass – Superfluid phase boundary, which corresponds to the vanishing of the superfluid stiffness.

We noted that a motivation for our work was the experiments by Choi *et al.* [61] on thermalization in the disordered two-dimensional BHM. In that work, there was an identification of a thermal to MBL transition at a critical disorder value of $\Delta/U = 5.3(2)$ when $U/J = 24.4$. Using these same parameter values, in Fig. 6, we show that this point appears to lie essentially at the Mott insulator – Bose glass phase transition identified in QMC simulations. While our calculations and the QMC calculations in Ref. [112] do not include a trap, this result adds further to the questions raised in Ref. [64] as to whether the experiments in Ref. [61] probe an MBL transition or a glass transition. We intend to explore this question further in future work on out-of-equilibrium dynamics of the disordered BHM.

CRediT authorship contribution statement

Ali Mokhtari-Jazi: Formal analysis, Methodology, Software, Validation, Visualization, Writing – original draft, Writing – review & editing. **Matthew R.C. Fitzpatrick:** Conceptualization, Formal analysis, Methodology, Software, Writing – original draft, Writing –

review & editing. **Malcolm P. Kennett:** Conceptualization, Formal analysis, Funding acquisition, Methodology, Supervision, Writing – review & editing.

Declaration of competing interest

The authors declare that they have no known competing financial interests or personal relationships that could have appeared to influence the work reported in this paper.

Data availability

No data was used for the research described in the article.

Acknowledgements

The authors thank NSERC for support of this work.

Appendix A. Propagator in the zero disorder and hopping limit

In the zero disorder and hopping limit, for an initial state $\hat{\rho}_i$ of the form given in Eq. (43), the spectral function $\mathcal{A}_{\vec{r}}(t)$ and the kinetic Green's function $\mathcal{G}^{(K)}_{\vec{r}}(t)$ can be expressed as follows:

$$\mathcal{G}^{(R)}_{\vec{r}}(t) = -i\Theta(t)\left\{\left(n_{\vec{r}}+1\right)e^{-i\left\{\mathcal{E}\left(\vec{r},n_{\vec{r}}+1\right)-\mathcal{E}\left(\vec{r},n_{\vec{r}}\right)\right\}t} - n_{\vec{r}}e^{i\left\{\mathcal{E}\left(\vec{r},n_{\vec{r}}-1\right)-\mathcal{E}\left(\vec{r},n_{\vec{r}}\right)\right\}t}\right\}, \tag{A.1}$$

$$\mathcal{G}^{(A)}_{\vec{r}}(t) = i\Theta(-t)\left\{\left(n_{\vec{r}}+1\right)e^{-i\left\{\mathcal{E}\left(\vec{r},n_{\vec{r}}+1\right)-\mathcal{E}\left(\vec{r},n_{\vec{r}}\right)\right\}t} - n_{\vec{r}}e^{i\left\{\mathcal{E}\left(\vec{r},n_{\vec{r}}-1\right)-\mathcal{E}\left(\vec{r},n_{\vec{r}}\right)\right\}t}\right\}, \tag{A.2}$$

$$\mathcal{G}^{(K)}_{\vec{r}}(t) = -i\left\{\left(n_{\vec{r}}+1\right)e^{-i\left\{\mathcal{E}\left(\vec{r},n_{\vec{r}}+1\right)-\mathcal{E}\left(\vec{r},n_{\vec{r}}\right)\right\}t} + n_{\vec{r}}e^{i\left\{\mathcal{E}\left(\vec{r},n_{\vec{r}}-1\right)-\mathcal{E}\left(\vec{r},n_{\vec{r}}\right)\right\}t}\right\}, \tag{A.3}$$

where $n_{\vec{r}}$ is particle density profile of the initial state, and

$$\mathcal{E}\left(\vec{r},n_{\vec{r}}\right) = \frac{U}{2}\sum_{\vec{r}} n_{\vec{r}}\left(n_{\vec{r}}-1\right) + \sum_{\vec{r}}\left(V_{\vec{r}}-\mu\right)n_{\vec{r}}. \tag{A.4}$$

Appendix B. Local quantities in the self-energy Σ^{zz}

In obtaining the effective self-energy Σ^{zz}_{δ}, we introduced two local quantities that are non-trivial functions of the initial particle density profile $n_{\vec{r}}$ and the chemical potential μ:

$$\mathcal{G}^{(R)}_{\vec{r},\omega\to 0} = -\frac{n_{\vec{r}}+1}{\mathcal{E}\left(\vec{r},n_{\vec{r}}+1\right)-\mathcal{E}\left(\vec{r},n_{\vec{r}}\right)} - \frac{n_{\vec{r}}}{\mathcal{E}\left(\vec{r},n_{\vec{r}}-1\right)-\mathcal{E}\left(\vec{r},n_{\vec{r}}\right)}, \tag{B.1}$$

and

$$\begin{aligned}\left[u_1\right]_{\vec{r}} = -2\left\{\mathcal{G}^{(R)}_{\vec{r},\omega\to 0}\right\}^{-4} &\times\left\{\frac{\left(n_{\vec{r}}+1\right)\left(n_{\vec{r}}+2\right)}{\left\{\mathcal{E}\left(\vec{r},n_{\vec{r}}+2\right)-\mathcal{E}\left(\vec{r},n_{\vec{r}}\right)\right\}\left\{\mathcal{E}\left(\vec{r},n_{\vec{r}}+1\right)-\mathcal{E}\left(\vec{r},n_{\vec{r}}\right)\right\}^2}\right.\\ &+\frac{n_{\vec{r}}\left(n_{\vec{r}}-1\right)}{\left\{\mathcal{E}\left(\vec{r},n_{\vec{r}}-2\right)-\mathcal{E}\left(\vec{r},n_{\vec{r}}\right)\right\}\left\{\mathcal{E}\left(\vec{r},n_{\vec{r}}-1\right)-\mathcal{E}\left(\vec{r},n_{\vec{r}}\right)\right\}^2}\\ &-\frac{\left(n_{\vec{r}}+1\right)^2}{\left\{\mathcal{E}\left(\vec{r},n_{\vec{r}}+1\right)-\mathcal{E}\left(\vec{r},n_{\vec{r}}\right)\right\}^3} - \frac{n_{\vec{r}}^2}{\left\{\mathcal{E}\left(\vec{r},n_{\vec{r}}-1\right)-\mathcal{E}\left(\vec{r},n_{\vec{r}}\right)\right\}^3}\\ &-\frac{n_{\vec{r}}\left(n_{\vec{r}}+1\right)}{\left\{\mathcal{E}\left(\vec{r},n_{\vec{r}}+1\right)-\mathcal{E}\left(\vec{r},n_{\vec{r}}\right)\right\}\left\{\mathcal{E}\left(\vec{r},n_{\vec{r}}-1\right)-\mathcal{E}\left(\vec{r},n_{\vec{r}}\right)\right\}^2}\\ &\left.-\frac{n_{\vec{r}}\left(n_{\vec{r}}+1\right)}{\left\{\mathcal{E}\left(\vec{r},n_{\vec{r}}+1\right)-\mathcal{E}\left(\vec{r},n_{\vec{r}}\right)\right\}^2\left\{\mathcal{E}\left(\vec{r},n_{\vec{r}}-1\right)-\mathcal{E}\left(\vec{r},n_{\vec{r}}\right)\right\}}\right\},\end{aligned} \tag{B.2}$$

where $\mathcal{E}\left(\vec{r},n_{\vec{r}}\right)$ is given by Eq. (A.4). Note that the expressions for $\mathcal{G}^{(R)}_{\vec{r},\omega\to 0}$ and $\left[u_1\right]_{\vec{r}}$ are very similar to those introduced in Ref. [92] for $\mathcal{G}^{12,(R)}(\omega\to 0)$ and u_1 respectively, with the biggest difference being the spatial dependence in the present case. In our numerical work, we do not consider a trap, and so u_1 can be taken to be independent of $\vec{r}$. We present the more general expression here for completeness.

Appendix C. Gapless spectrum in the HFBP approximation for the disordered-BHM

In this appendix, we extend the HFBP approximation presented in Ref. [93] to the disordered-BHM. In the SF phase, in order for the excitation spectrum to be gapless, we require that

$$\tilde{C}_{\vec{k}=0} = 0, \tag{C.1}$$

where $\tilde{C}_{\vec{k}}$ was defined in Eq. (133). Following the same approach as presented in Ref. [93], for $\tilde{C}_{\vec{k}=0}$ we obtain

$$\tilde{C}_{\vec{k}=0} = (U+\mu)^2 \left\{ \frac{\widetilde{\Delta}_\epsilon^2 \left(\check{G}^{12,(R)}_{\vec{k}=0}(\omega=0) - \check{G}^{22,(R)}_{\vec{k}=0}(\omega=0) \right)}{2} - 2u_1\phi^2 \right\} \times \left\{ \frac{\widetilde{\Delta}_\epsilon^2 \left(\check{G}^{12,(R)}_{\vec{k}=0}(\omega=0) + \check{G}^{22,(R)}_{\vec{k}=0}(\omega=0) \right)}{2} + u_1 \left\{ i\check{G}^{22,(K)}_{\vec{r}=0}(s=0) \right\} \right\}. \tag{C.2}$$

From Eq. (C.2) it is clear that to have Eq. (C.1) satisfied we should have

$$\check{G}^{22,(K)}_{\vec{r}=0}(s=0) = \frac{i\widetilde{\Delta}_\epsilon^2}{2u_1} \left(\check{G}^{12,(R)}_{\vec{k}=0}(\omega=0) + \check{G}^{22,(R)}_{\vec{k}=0}(\omega=0) \right). \tag{C.3}$$

Using the same procedure for $\check{G}^{11,(K)}_{\vec{r}=0}(s=0)$ we can write

$$\check{G}^{11,(K)}_{\vec{r}=0}(s=0) = \frac{i\widetilde{\Delta}_\epsilon^2}{2u_1} \left(\check{G}^{12,(R)}_{\vec{k}=0}(\omega=0) + \check{G}^{11,(R)}_{\vec{k}=0}(\omega=0) \right). \tag{C.4}$$

References

[1] P.W. Anderson, Absence of diffusion in certain random lattices, Phys. Rev. 109 (1958) 1492.
[2] D.M. Basko, I.L. Aleiner, B.L. Altshuler, Metal–insulator transition in a weakly interacting many-electron system with localized single-particle states, Ann. Phys. 321 (2006) 1126.
[3] D.A. Abanin, E. Altman, I. Bloch, M. Serbyn, Colloquium: many-body localization, thermalization, and entanglement, Rev. Mod. Phys. 91 (2019) 021001.
[4] V. Oganesyan, D.A. Huse, Localization of interacting fermions at high temperature, Phys. Rev. B 75 (2007) 155111.
[5] M. Žnidarič, T.c.v. Prosen, P. Prelovšek, Many-body localization in the Heisenberg XXZ magnet in a random field, Phys. Rev. B 77 (2008) 064426.
[6] A. Pal, D.A. Huse, Many-body localization phase transition, Phys. Rev. B 82 (2010) 174411.
[7] J.H. Bardarson, F. Pollmann, J.E. Moore, Unbounded growth of entanglement in models of many-body localization, Phys. Rev. Lett. 109 (2012) 017202.
[8] R. Vosk, E. Altman, Many-body localization in one dimension as a dynamical renormalization group fixed point, Phys. Rev. Lett. 110 (2013) 067204.
[9] M. Serbyn, Z. Papić, D.A. Abanin, Local conservation laws and the structure of the many-body localized states, Phys. Rev. Lett. 111 (2013) 127201.
[10] B. Bauer, C. Nayak, Area laws in a many-body localized state and its implications for topological order, J. Stat. Mech. 2013 (2013) P09005.
[11] J.A. Kjäll, J.H. Bardarson, F. Pollmann, Many-body localization in a disordered quantum Ising chain, Phys. Rev. Lett. 113 (2014) 107204.
[12] D.A. Huse, R. Nandkishore, V. Oganesyan, Phenomenology of fully many-body-localized systems, Phys. Rev. B 90 (2014) 174202.
[13] D. Pekker, G. Refael, E. Altman, E. Demler, V. Oganesyan, Hilbert-glass transition: new universality of temperature-tuned many-body dynamical quantum criticality, Phys. Rev. X 4 (2014) 011052.
[14] R. Nandkishore, D.A. Huse, Many-body localization and thermalization in quantum statistical mechanics, Annu. Rev. Condens. Matter Phys. 6 (2015) 15.
[15] S. Bera, H. Schomerus, F. Heidrich-Meisner, J.H. Bardarson, Many-body localization characterized from a one-particle perspective, Phys. Rev. Lett. 115 (2015) 046603.
[16] A. Chandran, I.H. Kim, G. Vidal, D.A. Abanin, Constructing local integrals of motion in the many-body localized phase, Phys. Rev. B 91 (2015) 085425.
[17] V. Ros, M. Müller, A. Scardicchio, Integrals of motion in the many-body localized phase, Nucl. Phys. B 891 (2015) 420.
[18] R. Vosk, D.A. Huse, E. Altman, Theory of the many-body localization transition in one-dimensional systems, Phys. Rev. X 5 (2015) 031032.
[19] A.C. Potter, R. Vasseur, S.A. Parameswaran, Universal properties of many-body delocalization transitions, Phys. Rev. X 5 (2015) 031033.
[20] D.A. Huse, Many-body localization needs a bath, Physics 9 (2016) 76.
[21] J.Z. Imbrie, Diagonalization and many-body localization for a disordered quantum spin chain, Phys. Rev. Lett. 117 (2016) 027201.
[22] J.Z. Imbrie, On many-body localization for quantum spin chains, J. Stat. Phys. 163 (2016) 998.
[23] L. Rademaker, M. Ortuño, Explicit local integrals of motion for the many-body localized state, Phys. Rev. Lett. 116 (2016) 010404.
[24] A.C. Potter, R. Vasseur, Symmetry constraints on many-body localization, Phys. Rev. B 94 (2016) 224206.
[25] L. Zhang, B. Zhao, T. Devakul, D.A. Huse, Many-body localization phase transition: a simplified strong-randomness approximate renormalization group, Phys. Rev. B 93 (2016) 224201.
[26] P.T. Dumitrescu, R. Vasseur, A.C. Potter, Scaling theory of entanglement at the many-body localization transition, Phys. Rev. Lett. 119 (2017) 110604.
[27] J.Z. Imbrie, V. Ros, A. Scardicchio, Local integrals of motion in many-body localized systems, Ann. Phys. (Berlin) 529 (2017) 1600278.
[28] R. Wortis, M.P. Kennett, Local integrals of motion in the two-site Anderson-Hubbard model, J. Phys. Condens. Matter 29 (2017) 405602.
[29] C. Monthus, Many-body-localization: strong disorder perturbative approach for the local integrals of motion, J. Phys. A, Math. Theor. 51 (2018) 195301.
[30] A. Goremykina, R. Vasseur, M. Serbyn, Analytically solvable renormalization group for the many-body localization transition, Phys. Rev. Lett. 122 (2019) 040601.
[31] B. Leipner-Johns, R. Wortis, Charge- and spin-specific local integrals of motion in a disordered Hubbard model, Phys. Rev. B 100 (2019) 125132.
[32] R.K. Panda, A. Scardicchio, M. Schulz, S.R. Taylor, M. Žnidarič, Can we study the many-body localisation transition?, Europhys. Lett. 218 (2019) 67003.
[33] S. Balasubramanian, Y. Liao, V. Galitski, Many-body localization landscape, Phys. Rev. B 101 (2020) 014201.
[34] M. Kiefer-Emmanouilidis, R. Unanyan, M. Fleischhauer, J. Sirker, Evidence for unbounded growth of the number entropy in many-body localized phases, Phys. Rev. Lett. 124 (2020) 243601.
[35] M. Tarzia, Many-body localization transition in Hilbert space, Phys. Rev. B 102 (2020) 014208.

[36] A. Morningstar, D.A. Huse, J.Z. Imbrie, Many-body localization near the critical point, Phys. Rev. B 102 (2020) 125134.
[37] S.J. Garratt, J.T. Chalker, Many-body delocalization as symmetry breaking, Phys. Rev. Lett. 127 (2021) 026802.
[38] K.S. Tikhonov, A.D. Mirlin, From Anderson localization on random regular graphs to many-body localization, Ann. Phys. 435 (2021) 168525.
[39] M. Kiefer-Emmanouilidis, R. Unanyan, M. Fleischhauer, J. Sirker, Slow delocalization of particles in many-body localized phases, Phys. Rev. B 103 (2021) 024203.
[40] M. Kiefer-Emmanouilidis, R. Unanyan, M. Fleischhauer, J. Sirker, Particle fluctuations and the failure of simple effective models for many-body localized phases, SciPost Phys. 12 (2022) 034.
[41] L. Fleishman, P.W. Anderson, Interactions and the Anderson transition, Phys. Rev. B 21 (1980) 2366.
[42] B.L. Altshuler, Y. Gefen, A. Kamenev, L.S. Levitov, Quasiparticle lifetime in a finite system: a nonperturbative approach, Phys. Rev. Lett. 78 (1997) 2803.
[43] I.V. Gornyi, A.D. Mirlin, D.G. Polyakov, Interacting electrons in disordered wires: Anderson localization and low-T transport, Phys. Rev. Lett. 95 (2005) 206603.
[44] D.J. Luitz, N. Laflorencie, F. Alet, Many-body localization edge in the random-field Heisenberg chain, Phys. Rev. B 91 (2015) 081103(R).
[45] B. Villalonga, X. Yu, D.J. Luitz, B.K. Clark, Exploring one-particle orbitals in large many-body localized systems, Phys. Rev. B 97 (2018) 104406.
[46] A. Chandran, A. Pal, C.R. Laumann, A. Scardicchio, Many-body localization beyond eigenstates in all dimensions, Phys. Rev. B 94 (2016) 144203.
[47] Y.B. Lev, D.R. Reichman, Slow dynamics in a two-dimensional Anderson-Hubbard model, Europhys. Lett. 113 (2016) 46001.
[48] K. Agarwal, E. Altman, E. Demler, S. Gopalakrishnan, D.A. Huse, M. Knap, Rare-region effects and dynamics near the many-body localization transition, Ann. Phys. (Berlin) 529 (2017) 1600326.
[49] W. De Roeck, F. Huveneers, Stability and instability towards delocalization in many-body localization systems, Phys. Rev. B 95 (2017) 155129.
[50] W. De Roeck, J.Z. Imbrie, Many-body localization: stability and instability, Phil. Trans. R. Soc. A 375 (2017) 20160422.
[51] S.J. Thomson, M. Schiró, Time evolution of many-body localized systems with the flow equation approach, Phys. Rev. B 97 (2018) 060201(R).
[52] S. Gopalakrishnan, D.A. Huse, Instability of many-body localized systems as a phase transition in a nonstandard thermodynamic limit, Phys. Rev. B 99 (2019) 134305.
[53] T. Wahl, A. Pal, S. Simon, Signatures of the many-body localized regime in two dimensions, Nat. Phys. 15 (2019) 164.
[54] E.V.H. Doggen, I.V. Gornyi, A.D. Mirlin, D.G. Polyakov, Slow many-body delocalization beyond one dimension, Phys. Rev. Lett. 125 (2020) 155701.
[55] H. Théveniaut, Z. Lan, G. Meyer, F. Alet, Transition to a many-body localized regime in a two-dimensional disordered quantum dimer model, Phys. Rev. Res. 2 (2020) 033154.
[56] A. Kshetrimayum, M. Goihl, J. Eisert, Time evolution of many-body localized systems in two spatial dimensions, Phys. Rev. B 102 (2020) 235132.
[57] E. Chertkov, B. Villalonga, B.K. Clark, Numerical evidence for many-body localization in two and three dimensions, Phys. Rev. Lett. 126 (2021) 180602.
[58] F. Pietracarina, F. Alet, Probing many-body localization in a disordered quantum dimer model on the honeycomb lattice, SciPost Phys. 10 (2021) 044.
[59] S.S. Kondov, W.R. McGehee, W. Xu, B. DeMarco, Disorder-induced localization in a strongly correlated atomic Hubbard gas, Phys. Rev. Lett. 114 (2015) 083002.
[60] M. Schreiber, S.S. Hodgman, P. Bordia, H.P. Lüschen, M.H. Fischer, R. Vosk, E. Altman, U. Schneider, I. Bloch, Observation of many-body localization of interacting fermions in a quasirandom optical lattice, Science 349 (2015) 842.
[61] J.-Y. Choi, S. Hild, J. Zeiher, P. Schauß, A. Rubio-Abadal, T. Yefsah, V. Khemani, D.A. Huse, I. Bloch, C. Gross, Exploring the many-body localization transition in two dimensions, Science 352 (2016) 1547.
[62] P. Bordia, H. Lüschen, S. Scherg, S. Gopalakrishnan, M. Knap, U. Schneider, I. Bloch, Probing slow relaxation and many-body localization in two-dimensional quasiperiodic systems, Phys. Rev. X 7 (2017) 041047.
[63] H.P. Lüschen, P. Bordia, S. Scherg, F. Alet, E. Altman, U. Schneider, I. Bloch, Observation of slow dynamics near the many-body localization transition in one-dimensional quasiperiodic systems, Phys. Rev. Lett. 119 (2017) 260401.
[64] M. Yan, H.-Y. Hui, M. Rigol, V.W. Scarola, Equilibration dynamics of strongly interacting bosons in 2D lattices with disorder, Phys. Rev. Lett. 119 (2017) 073002.
[65] M. Greiner, O. Mandel, T. Esslinger, T.W. Hänsch, I. Bloch, Collapse and revival of the matter wave field of a Bose-Einstein condensate, Nature 415 (2002) 39.
[66] I. Bloch, Ultracold quantum gases in optical lattices, Nat. Phys. 1 (2005) 23.
[67] D. Jaksch, P. Zoller, The cold atom Hubbard toolbox, Ann. Phys. 315 (2005) 52.
[68] M. Lewenstein, A. Sanpera, V. Ahufinger, B. Damski, A. Sen, U. Sen, Ultracold atomic gases in optical lattices: mimicking condensed matter physics and beyond, Adv. Phys. 56 (2007) 243.
[69] I. Bloch, J. Dalibard, W. Zwerger, Many-body physics with ultracold gases, Rev. Mod. Phys. 80 (2008) 885.
[70] C.-L. Hung, X. Zhang, N. Gemelke, C. Chin, Slow mass transport and statistical evolution of an atomic gas across the superfluid–Mott-insulator transition, Phys. Rev. Lett. 104 (2010) 160403.
[71] W.S. Bakr, A. Peng, M.E. Tai, R. Ma, J. Simon, J.I. Gillen, S. Fölling, L. Pollet, M. Greiner, Probing the superfluid-to-Mott insulator transition at the single-atom level, Science 329 (2010) 547.
[72] M.P. Kennett, Out-of-equilibrium dynamics of the Bose-Hubbard model, ISRN Condens. Matter Phys. 2013 (2013) 393616.
[73] C. Gross, I. Bloch, Quantum simulations with ultracold atoms in optical lattices, Science 357 (2017) 995.
[74] S.R. Clark, D. Jaksch, Dynamics of the superfluid to Mott-insulator transition in one dimension, Phys. Rev. A 70 (2004) 043612.
[75] C. Kollath, A.M. Läuchli, E. Altman, Quench dynamics and nonequilibrium phase diagram of the Bose-Hubbard model, Phys. Rev. Lett. 98 (2007) 180601.
[76] A.M. Läuchli, C. Kollath, Spreading of correlations and entanglement after a quench in the one-dimensional Bose–Hubbard model, J. Stat. Mech. 5 (2008) 05018.
[77] J.-S. Bernier, G. Roux, C. Kollath, Slow quench dynamics of a one-dimensional Bose gas confined to an optical lattice, Phys. Rev. Lett. 106 (2011) 200601.
[78] M. Cheneau, P. Barmettler, D. Poletti, M. Endres, P. Schauß, T. Fukuhara, C. Gross, I. Bloch, C. Kollath, S. Kuhr, Light-cone-like spreading of correlations in a quantum many-body system, Nature 481 (2012) 484.
[79] P. Barmettler, D. Poletti, M. Cheneau, C. Kollath, Propagation front of correlations in an interacting Bose gas, Phys. Rev. A 85 (2012) 053625.
[80] S. Trotzky, Y.-A. Chen, A. Flesch, I.P. McCulloch, U. Schollwöck, J. Eisert, I. Bloch, Probing the relaxation towards equilibrium in an isolated strongly correlated one-dimensional Bose gas, Nat. Phys. 8 (2012) 325.
[81] J.-S. Bernier, D. Poletti, P. Barmettler, G. Roux, C. Kollath, Slow quench dynamics of Mott-insulating regions in a trapped Bose gas, Phys. Rev. A 85 (2012) 033641.
[82] L. Cevolani, J. Despres, G. Carleo, L. Tagliacozzo, L. Sanchez-Palencia, Universal scaling laws for correlation spreading in quantum systems with short- and long-range interactions, Phys. Rev. B 98 (2018) 024302.
[83] J. Despres, L. Villa, L. Sanchez-Palencia, Twofold correlation spreading in a strongly correlated lattice Bose gas, Sci. Rep. 9 (2019) 4135.
[84] P. Navez, R. Schützhold, Emergence of coherence in the Mott-insulator–superfluid quench of the Bose-Hubbard model, Phys. Rev. A 82 (2010) 063603.
[85] C. Trefzger, K. Sengupta, Nonequilibrium dynamics of the Bose-Hubbard model: a projection-operator approach, Phys. Rev. Lett. 106 (2011) 095702.
[86] K.V. Krutitsky, P. Navez, F. Queisser, R. Schützhold, Propagation of quantum correlations after a quench in the Mott-insulator regime of the Bose-Hubbard model, Eur. Phys. J. Quantum Technol. 1 (2014) 12.
[87] F. Queisser, K.V. Krutitsky, P. Navez, R. Schützhold, Equilibration and prethermalization in the Bose-Hubbard and Fermi-Hubbard models, Phys. Rev. A 89 (2014) 033616.
[88] G. Carleo, F. Becca, L. Sanchez-Palencia, S. Sorella, M. Fabrizio, Light-cone effect and supersonic correlations in one- and two-dimensional bosonic superfluids, Phys. Rev. A 89 (2014) 031602.

[89] Y. Yanay, E.J. Mueller, Evolution of coherence during ramps across the Mott-insulator–superfluid phase boundary, Phys. Rev. A 93 (2016) 013622.
[90] R. Kaneko, I. Danshita, Tensor-network study of correlation-spreading dynamics in the two-dimensional Bose-Hubbard model, Commun. Phys. 5 (2022) 65.
[91] M.P. Kennett, D. Dalidovich, Schwinger-Keldysh approach to out-of-equilibrium dynamics of the Bose-Hubbard model with time-varying hopping, Phys. Rev. A 84 (2011) 033620.
[92] M.R.C. Fitzpatrick, M.P. Kennett, Contour-time approach to the Bose-Hubbard model in the strong coupling regime: studying two-point spatio- temporal correlations at the Hartree-Fock-Bogoliubov level, Nucl. Phys. B 930 (2018) 1.
[93] M.R.C. Fitzpatrick, M.P. Kennett, Light-cone-like spreading of single-particle correlations in the Bose-Hubbard model after a quantum quench in the strong-coupling regime, Phys. Rev. A 98 (2018) 053618.
[94] M.R.C. Fitzpatrick, Out-of-equilibrium dynamics of the Bose-Hubbard model in the strong coupling regime, Ph.D. thesis, Simon Fraser University, 2019.
[95] M.P. Kennett, M.R.C. Fitzpatrick, Spatio-temporal spreading of correlations in the Bose–Hubbard model, J. Low Temp. Phys. 201 (2020) 82.
[96] A. Mokhtari-Jazi, M.R.C. Fitzpatrick, M.P. Kennett, Phase and group velocities for correlation spreading in the Mott phase of the Bose-Hubbard model in dimensions greater than one, Phys. Rev. A 103 (2021) 023334.
[97] Y. Takasu, T. Yagami, H. Asaka, Y. Fukushima, K. Nagao, S. Goto, I. Danshita, Y. Takahashi, Energy redistribution and spatiotemporal evolution of correlations after a sudden quench of the Bose-Hubbard model, Sci. Adv. 6 (2020) eaba9255.
[98] M.P.A. Fisher, P.B. Weichman, G. Grinstein, D.S. Fisher, Boson localization and the superfluid-insulator transition, Phys. Rev. B 40 (1989) 546.
[99] J.K. Freericks, H. Monien, Strong-coupling expansions for the pure and disordered Bose-Hubbard model, Phys. Rev. B 53 (1996) 2691.
[100] M. Rispoli, A. Lukin, R. Schittko, S. Kim, M.E. Tai, J. Léonard, M. Greiner, Quantum critical behaviour at the many-body localization transition, Nature 573 (2019) 385.
[101] R. Yao, J. Zakrzewski, Many-body localization in the Bose-Hubbard model: evidence for mobility edge, Phys. Rev. B 102 (2020) 014310.
[102] S.W. Kim, G. De Tomasi, M. Heyl, Real-time dynamics of one-dimensional and two-dimensional bosonic quantum matter deep in the many-body localized phase, Phys. Rev. B 104 (2021) 144205.
[103] J. Chen, X. Wang, Many-body localization in a disorder Bose-Hubbard chain, arXiv:2104.08582v2, 2021.
[104] L. Villa, S.J. Thomson, L. Sanchez-Palencia, Finding the phase diagram of strongly correlated disordered bosons using quantum quenches, Phys. Rev. A 104 (2021) 023323.
[105] C.-H. Lin, R. Sensarma, K. Sengupta, S. Das Sarma, Quantum dynamics of disordered bosons in an optical lattice, Phys. Rev. B 86 (2012) 214207.
[106] S.J. Thomson, L.S. Walker, T.L. Harte, G.D. Bruce, Measuring the Edwards-Anderson order parameter of the Bose glass: a quantum gas microscope approach, Phys. Rev. A 94 (2016) 051601(R).
[107] C. Meldgin, U. Ray, P. Russ, D. Chen, D.M. Ceperley, B. DeMarco, Probing the Bose glass–superfluid transition using quantum quenches of disorder, Nat. Phys. 12 (2016) 646.
[108] G. Bertoli, B.L. Altshuler, G.V. Shlyapnikov, Many-body localization in continuum systems: two-dimensional bosons, Phys. Rev. A 100 (2019) 013628.
[109] A. Geißler, G. Pupillo, Mobility edge of the two-dimensional Bose-Hubbard model, Phys. Rev. Res. 2 (2020) 042037(R).
[110] A. Geißler, Finite-size scaling analysis of localization transitions in the disordered two-dimensional Bose-Hubbard model within the fluctuation operator expansion method, Phys. Rev. A 103 (2021) 043332.
[111] R.S. Souza, A. Pelster, F.E.A. dos Santos, Green's function approach to the Bose–Hubbard model with disorder, New J. Phys. 23 (2021) 083007.
[112] S.G. Söyler, M. Kiselev, N.V. Prokof'ev, B.V. Svistunov, Phase diagram of the commensurate two-dimensional disordered Bose-Hubbard model, Phys. Rev. Lett. 107 (2011) 185301.
[113] V. Gurarie, L. Pollet, N.V. Prokof'ev, B.V. Svistunov, M. Troyer, Phase diagram of the disordered Bose-Hubbard model, Phys. Rev. B 80 (2009) 214519.
[114] K. Sengupta, N. Dupuis, Mott-insulator–to–superfluid transition in the Bose-Hubbard model: a strong-coupling approach, Phys. Rev. A 71 (2005) 033629.
[115] J. Schwinger, Brownian motion of a quantum oscillator, J. Math. Phys. 2 (1961) 407.
[116] L.V. Keldysh, Diagram technique for nonequilibrium processes, Zh. Eksp. Teor. Fiz. 20 (1964) 1515, Sov. Phys. JETP 20 (1965) 1018.
[117] J. Rammer, H. Smith, Quantum field-theoretical methods in transport theory of metals, Rev. Mod. Phys. 58 (1986) 323.
[118] A.J. Niemi, G.W. Semenoff, Finite-temperature quantum field theory in Minkowski space, Ann. Phys. 152 (1984) 105.
[119] N.P. Landsman, C.G. van Weert, Real- and imaginary-time field theory at finite temperature and density, Phys. Rep. 145 (1987) 141.
[120] K.-c. Chou, Z.-b. Su, B.-l. Hao, L. Yu, Equilibrium and nonequilibrium formalisms made unified, Phys. Rep. 118 (1985) 1.
[121] A. Kamenev, A. Andreev, Electron-electron interactions in disordered metals: Keldysh formalism, Phys. Rev. B 60 (1999) 2218.
[122] C. Chamon, A.W.W. Ludwig, C. Nayak, Schwinger-Keldysh approach to disordered and interacting electron systems: derivation of Finkelstein's renormalization-group equations, Phys. Rev. B 60 (1999) 2239.
[123] J.W. Negele, H. Orland, Quantum Many Particle Systems, Addison-Wesley, Reading, MA, 1998.
[124] J.M. Cornwall, R. Jackiw, E. Tomboulis, Effective action for composite operators, Phys. Rev. D 10 (1974) 2428.
[125] M.P. Kennett, C. Chamon, J. Ye, Aging dynamics of quantum spin glasses of rotors, Phys. Rev. B 64 (2001) 224408.
[126] N. Dupuis, A new approach to strongly correlated fermion systems: the spin–particle–hole coherent-state path integral, Nucl. Phys. B 618 (2001) 617.
[127] S. Pairault, D. Sénéchal, A.-M.S. Tremblay, Superperturbation solver for quantum impurity models, Eur. Phys. J. B 16 (2000) 85.
[128] V.N. Popov, Functional Integrals in Quantum Field Theory and Statistical Physics, Springer, Dordrecht, 1983.